

1 Authors response

2 Gong et al

3

4 We are grateful to two anonymous reviewers that had put a lot of effort to improve our  
5 manuscript. Accordingly, we did our best to follow the suggestions. In those few cases where we  
6 disagreed or were not able to follow suggestions, we explain why. Please find our responses to  
7 each comment below.

8

9 The revised manuscript where changes are done using *Word track change function* are located  
10 in the end after the comments from referees and our responses.

11

12 Referee 1

13

14 General comments

15

16 1. Please provide a list of abbreviations! It was hard work trying to follow the methods  
17 and results without one.

18

19 R: We now provide a list of symbols and abbreviations as suggested (new Table 1).

20

21 2. A discussion of some literature very relevant to this study, exploring the same ideas though  
22 without using a formal model, is missing:

23 (Titus, et al. 1983, Titus and Wagner 1984). One of the interesting results of these studies is that  
24 there is a seasonal dynamic in the water-content response of photosynthesis. This may be very  
25 relevant to your model, if the model is sensitive to these 0water-stress0 responses.

26 (Rydin 1986, 1993a, b, 1997, Rydin and Barber 2001) And more: check the publications by Hakan  
27 Rydin, he has been working on competition between Sphagna for along time.

28

29 Another important source, which, however, has not yet been fully published (but a relevant  
30 summary with numbers to compare yours against is available in the thesis summary:  
31 <http://www.diva-portal.org/smash/get/diva2:1282760/FULLTEXT01.pdf> ), is the recent PhD  
32 thesis by Fia Bengtsson (Uppsala), in particular chapters 4 and 5.

33 This paper (Hájek 2014) is also very relevant, among other things for some methodological issues.

34

35 R: Thank you for pointing out missing references to relevant literature. Indeed we  
36 were missing quite a number of classics and new ones that are now used to deepen  
37 Intro and Discussion. Originally, we presented model development and empirical  
38 measurements in two separate manuscripts; In the merging we had accidentally  
39 lost a big part of references but now they are included again.

40

41 3. Model structure: The abstract promises a very wide scope (0dynamic feedback between plant  
42 community structure and the environment0), but there is no feedback from the species  
43 composition (Modules 1 and 2) on the hydrology (module 3) in the model. Therefore: how does

44 this model really address the feedback you mention?  
45

46 R: Our model lacks the feedback to hydrology as the referee pointed out. We now  
47 removed the parts of Abstract and Introduction that give reader a reason to expect  
48 otherwise.  
49

50 In the discussion, you could also be more explicit about the implications of the species  
51 composition on biogeochemical processes, see e.g. (Bengtsson, et al. 2016, Cornelissen, et al.  
52 2007). Alternatively, do not suggest this focus on feedbacks in the abstract and introduction.  
53

54 R: In the discussion we now describe the implications of the species composition on  
55 biogeochemical processes via their traits.  
56

57 The vertical water transport is implemented in detail, but in the detailed modules 1 and 2 there  
58 does not seem to be horizontal water exchange between neighbours, although this may play an  
59 important role in maintaining Sf in hummocks, supported by the water held in Sm (Rydin 1985 ;  
60 Rydin and McDonald 1985 ; Robroek et al. 2007a ). In your experiments, basing the drying speed  
61 on single capitula, the capitulum density, i.e. facilitation between neighbours in retaining water,  
62 could not affect the drying speed, thereby possibly missing part of the difference between the  
63 lawn and the hummock species (i.e. under-estimating the difference).  
64

65 R: Our model also lacks horizontal water transport that has found to allow  
66 individuals of lawn species to be present in dried habitats. The pattern is interesting  
67 and may play a role in speeding up the spreading of lawn species when conditions  
68 become wetter. Unfortunately, in this first attempt to mechanistically model  
69 Sphagnum community dynamics we were only able focus getting the general  
70 distribution pattern realistic and leave perfection for later. In this stage essential  
71 data for parameter values not yet exist for quantifying horizontal water transport  
72 among neighboring individuals such as hydraulic conductivity. The model can be  
73 improved further when the parameterization could be supported by experimental  
74 studies.  
75

76 In our drying experiment a layer of capitula, with same density as in field was placed  
77 on the cuvette, therefor the neighbours do to some extend affect the drying  
78 process, yet, the stems are lacking and it surely does not truly reflect the field  
79 conditions.  
80

81 Speed as such was not yet our focus but the response of photosynthesis to water  
82 content, and we do think our approach catches the between species differences in  
83 this process.  
84

85 4. Model parameters / results L487 & L520-522 Please also explain why Sf has an advantage over  
86 Sm in the lawns. Why does Sf have faster growth? This is not clear to me at all. According to your

87 photosynthesis measurements, Sf has a lower Amax (which seems strange, usually indeed lawn  
88 species have higher rates) and the same respiration rate as Sm. Therefore, at high water content  
89 and high light, Sm and not Sf should have a benefit in terms of NSC production. As the conversion  
90 from NSC to biomass is the same for both species, the only way to explain the higher length  
91 growth of Sf in the lawn environment is the higher Hspc (higher height growth per unit biomass).  
92 Correct?

93

94 R: The explanation suggested by the Refree 1 is correct. We have now written out  
95 that the bigger height growth of *S. fallax* per biomass production rate is because of  
96 its looser structure. Like us, Bengtson et al. (2016) measured similar photosynthesis  
97 rate for the two species, but clearly higher height growth for *S. fallax*. (Bengtsson,  
98 F., Granath, G., & Rydin, H. (2016). Photosynthesis, growth, and decay traits in  
99 *Sphagnum* – a multispecies comparison. *Ecology and Evolution*, 6(10), 3325-3341.)

100 5. Ecophysiological measurements / model parameters: L1017 You state here that A tended to  
101 increase with time and that it peaked at water contents below the maximum, as indeed shown  
102 by the theoretical figure 1B, but not by the measured curves in Fig 2C. Indeed I would have  
103 expected such a peak. Can you explain the absence of diffusion limitation in your experiment?  
104 Good ventilation..? Is it realistic to measure one capitulum in isolation? Lots of air all around it  
105 compared to a capitulum immersed in a (wet) *Sphagnum* mat: : : Consequently, also, how  
106 homogenously will the capitula have dried out in the GFS compared to in a *Sphagnum* mat?

107

108 R: The expected peak was actually there, see redrawn figure B2C. For some reason  
109 (not clear to us anymore) we had earlier cut the X-axis (capitulum water content)  
110 shorter in panel C than in the other panels.

111

112 We did not measure single capitulum in isolation but a layer of capitula was placed  
113 on cuvette (see Fig. B1A). We rewrote the related methods section to make them  
114 clearer.

115

116 It has been shown that the speed of drying during gas exchange measurements can strongly  
117 affect the conclusions about optimum water content and water compensation point (Hájek  
118 2014). Under quick drying, as in your experiments, it seems typical to get the type of curves you  
119 present. However, under slower drying, as would be typical in the field, the optimum WC would  
120 be lower and the depression at high WC stronger. In particular the high compensation point you  
121 found, at water contents of up to 600%, seems to be a typical artefact of such fast drying, related  
122 to the inhomogenous drying within the capitula.

123

124 R: In slow drying (Hájek 2014), environmental vapor pressure remains constant and  
125 evaporation rate decreases with time. In such experimental conditions water  
126 movement could be sufficiently rebalanced between internal and external tissues,  
127 so that the water potential becomes equilibrated among different parts of  
128 capitulum. However, in field conditions, evaporation demand could be more  
129 strongly driven by radiation than vapor pressure deficit, particularly during a hot

130 clear summer day. Thus, it could be much faster than in a desiccation chamber and  
131 consequently, the water content may not rebalance fast enough to reach  
132 equilibrium. Moreover, the branch leaves in the outer part of capitula could be  
133 more photosynthetically active than the internal core parts. As the drying is  
134 heterogenous, photosynthesis rate could be largely reduced just by the drying of  
135 outer tissues, even though the internal core part could be wetter. This is also  
136 supported by our measurement, which showed a higher compensation point for  
137 photosynthesis than that from the slow drying experiment (Hájek 2014). Therefore,  
138 we believe the fast drying could be a better imitation of field processes.  
139

140 Also, a field water content of 1470 and 809% water per dry mass seems extremely low for  
141 Sphagnum in general and for these species. For *S. magellanicum* I have seen max WC values  
142 reported between 2000 and 3000%, and for *S. fallax* of about 1500% (or 1100%, equivalent to 12  
143 gFM/gDM (Titus, et al. 1983)). You even state yourself (Line270) that it is known that Wmax is  
144 around 25-30 g g<sup>-1</sup>. So I do not understand why you started your experiment at 14,7 and 8,09 g  
145 g<sup>-1</sup> or where you use these values, as opposed to the values in L277.  
146

147 R: The reason for the low field water contents compared to earlier published values  
148 lies in the measurement method we used (as explained in supplementary material).  
149 We measured the capitulum and stem section WC separately and allowed the  
150 external water on *Sphagnum* surfaces to dry out before weighing the fresh weight.  
151 We started the experiment on the water content levels where excess water does  
152 not limit photosynthesis. This optimal WC is now shown in redrawn Figure B2C,  
153 which now starts already in a higher water content. We have now tried to explain  
154 this better in Methods.  
155

156 If the light curves took up to 120 minutes to complete (why? That is a very long time especially if  
157 you only measured at 4 light levels, which seems very little to determine a reliable curve: : :), and  
158 drying down to the compensation point took 120-180 minutes, this implies that during the light  
159 response measurements you measured a combination of reduced light and reduced water  
160 content, so that the curves probably do not reflect only the light response. For determining the  
161 Amax this should be no problem, as you started at the highest light level, i.e. at Amax. Are you  
162 sure there was no photoinhibition at these high light levels? This may be a problem when starting  
163 light response  
164 measurements at the high end, as it would affect the rest of the measurements.  
165

166 R: It is true that the light response curve cannot exclude the impact of drying. To  
167 mitigate the impact, we have measured the photosynthesis at highest light level  
168 from the beginning of each measurement, then decreased the light level  
169 sequentially (as respiration could be less sensitive to drying).  
170

171 We have added more details on the measurement protocol and choice of light  
172 levels. The cuvette relative humidity was kept at 80% to slow down the drying  
173 process, but not to cause damage to the device. The maximum light level 1500 PPFD

174 was chosen based on our earlier studies with more light levels (Laine 2011, 2015)  
175 where we had not observed any photoinhibition until PPFD 2000, and A were often  
176 still increasing between PPFD 800 and 1500.

177 Laine, A. M., Juurola, E., Hájek, T., & Tuittila, E. S.: Sphagnum growth and ecophysiology during mire  
178 succession. *Oecologia*, 167(4), 1115-1125, 2011.

179 Laine, A. M., Ehonen, S., Juurola, E., Mehtätalo, L., & Tuittila, E. S.: Performance of late succession  
180 species along a chronosequence: Environment does not exclude *Sphagnum fuscum* from the early  
181 stages of mire development. *Journal of vegetation science*, 26(2), 291-301, 2015.

182

183 6. Model tests: As an important difference between your and previous models lies in the coupling  
184 to environmental fluctuations and stochasticity (L97-98), it would make sense to present a test  
185 of the importance of these processes to the model output. Would a simpler model provide  
186 similarly good results?

187

188 R: We believe that the main purpose of modelling is to illustrate the reality and  
189 serve as a tool for systematic assessment of the processes. Simple community  
190 models without individual-based processes implicitly weigh on generality and  
191 forgive outliers. However, environmental fluctuation and extremes are becoming  
192 more frequent and intensive with climate change, and this is likely to give  
193 advantage to an otherwise unlikely change in peatland community. To help with  
194 this situation, our modelling is able to populate outputs along a probability  
195 distribution and allows assessing individuals with different trait combinations as a  
196 part of the probabilities. As these models are fundamentally different in focuses  
197 and underlying mechanisms, simply comparing the goodness of results seems  
198 pointless.

199

200 I would also be interested in seeing the effects of the water retention and photosynthetic water-  
201 response parameters separately. Especially since the parameters for the latter may suffer from  
202 some measurement artefacts.

203

204 R: This is a very appreciated comment. Our future goal is also to make the picture  
205 clearer and understanding the factorial effects is a very important aspect. At the  
206 moment, our data and techniques are insufficient to separate the different effects.  
207 Therefore, model testing based on the parameters quantified by the "mixed"  
208 information could be less informative, unless we have had improved measurement  
209 data.

210

211 In addition, *S. fallax* and *S. magellanicum* are largely different in both water  
212 retention and photosynthetic response to water stress. Further testing on species  
213 either with similar water retention, or with similar photosynthetic response would  
214 be more informative to this question.

215

216

217

218 7. Presentation: L279-352 are all about module 3, which seems a bit unbalanced, seeing that

219 modules 1 and 2 seem more important for the competition results. Model 3 is not tested in this  
220 paper:

221

222 R: Module 3 is about environment and it was not tested here because it was not in  
223 the focus of this paper. However, to bridge environmental fluctuation to  
224 community processes, our center of the focus, we needed to set up the  
225 environment first.

226

227

228 Specific comments

229

230 L20 In the introduction it could be explained more clearly why a mechanistic model I needed to  
231 predict species compositions under changing water levels. Is a prediction based on known habitat  
232 preferences not good enough?

233

234 R: The species known preference along the prevailing moisture gradient might not  
235 directly serve as a reliable predictor for future species compositions as water table  
236 fluctuation is likely to increase. This is now added in Introduction.

237

238

239 L60-61 how does the species composition affect these processes? In particular (for discussion),  
240 how do your species / ecological types affect these processes?

241

242 R: through interspecific variability in species traits such as photosynthetic potential  
243 and litter quality

244

245

246 L381 it would be interesting to see the effects of water retention and water stress separately

247

248 R: See above the response to 6

249

250

251 L471 to me it does not look like photosynthesis of *S. fallax* is more sensitive to changes in the  
252 water content, as *Amax* lies at lower water contents than for *S. magellanicum*, suggesting that it  
253 can handle dry conditions better.

254

255 R: In this study, we use the term sensitivity to represent the dependency of  
256 photosynthesis changes to water content changes in capitula. Although *S. fallax* has  
257 greater tolerance to relatively low water content, the water content change for  
258 photosynthesis to drop from maximum to zero was much smaller than *S.*  
259 *magellanicum* (B2C). This is why we claim that photosynthesis of *S. fallax* is more  
260 sensitive to changes in the water content. This is now better pointed out in the text.

261

262

263 L552 how exactly may it serve?

264

265 R: we have removed the sentence

266

267

268 L561 Similarly, how could it be used in DVM development? If you can, please try to be more  
269 explicit here.

270

271 R: We introduced a mechanism to include competition based on growth rates that  
272 could be used in building dynamic community structure into DVMs.

273

274

275 Table 1: Rs20 was not significantly different between the species, then why use different values  
276 here? How large is the effect on the results?

277

278 R: These values are measured from field experiments and reported here. Although  
279 the means are not significantly different, we cannot judge that the probability  
280 distributions are the same, based on only several samples. Therefore, we used the  
281 measured means and standard deviations to generate probability distributions for  
282 each species.

283

284

285 Technical corrections:

286

287 L24 employs

288

289 R: corrected

290

291 L50 why “during decadal timeframe”?

292

293 R: not within few years but faster than a hundred yeas

294

295 L57 have

296

297 R: corrected

298

299 L66 remove “community”

300

301 R: removed

302

303 L69 I do not think that this modelling can be considered a “space-for-time” approach. The  
304 processes are different in space than in time.

305

306 R: removed

307  
308 L90 : : :that is covered: : ;, : : :As competition occurs: : :  
309  
310 R: modified as suggested  
311  
312 L100 within the peatland moss layer  
313  
314 R: added  
315  
316 L102 whose competitiveness?  
317  
318 R: clarified  
319  
320 L106 positions a long a  
321  
322 R: corrected  
323  
324 L113 modelled is located  
325  
326 R: modified as suggested  
327  
328 L119 with a sparse cover of vascular plants  
329  
330 R: modified as suggested  
331  
332 L125 The Peatland: : :  
333  
334 R: added  
335  
336 L126 explain “water-energy conditions”  
337  
338 R: clarified  
339  
340 L128 consisting  
341  
342 R: modified  
343  
344 L132 are driven  
345  
346 R: modified  
347  
348 L142-143 A is not directly controlled by CWR, please rephrase  
349  
350 R: rephrased



351  
352 L145 These were not really random variables, but variables randomly selected from a distribution  
353  
354 R: corrected  
355  
356 Eq5: what are the rules for the timing of growth? Any relation to WC?  
357  
358 R: Timing of growth is controlled by a temperature threshold and NSC availability. Growth occurs  
359 when  $T > 5$  °C and NSC is above zero. The dynamics of NSC storage is related to WC through net  
360 photosynthesis.  
361  
362 L191 explain where Kimm is based on  
363  
364 R: Reference added to Asaeda, T. and Karunaratne (2000)  
365  
366 Asaeda, T. and Karunaratne, S.: Dynamic modelling of the growth of *Phragmites australis*: model description, *Aquatic*  
367 *Botany*, 67, 301-318, 2000.  
368  
369 L204 ii) biomass, or NSC?  
370  
371 R: NSC; corrected  
372  
373 L212 This order of sentences suggests that an exhaustion of NSC storage would be due to lateral  
374 growth, which would not make sense, as lateral growth should not take place if NSC supplies are  
375 not enough to sustain both new capitula  
376  
377 R: Indeed, it does not make sense. Removed  
378  
379 L217 why suddenly “moss parameters’ - better use the same terms all the time  
380  
381 R: reformulated  
382  
383 L227 how does shoot density vary in the model, if you model one capitulum per grid cell?  
384  
385 R:  $D_s$  is BM per grid cell, not the number of capitula. The (suggested) table of abbreviations with their  
386 units will clarify this.  
387  
388 L235 where is the centre of the moss layer?  
389  
390 R: removed  
391  
392 L239 what is the  $O_{capacity}$  of water?  
393  
394 R: corrected to “water uptake capacity”  
395

396 L264 0where  $W_{opt}$  is the optimal water: : :  
397  
398 R: reformulated  
399  
400 L270-278 It is not clear to me why this equation was needed.  
401  
402 R: In Eq. 11 we evaluated the water stress effect at high  $W_{cap}$  conditions, which are beyond the  
403 upper boundary of our drying experiment. Therefore in Eq. 12 we used a brief method to  
404 estimate the capitula  $W_{cap}$  from volumetric water content of moss carpet.  
405  
406 L277 Is the same  $W_{max}$  used for both species..? An how about the values in Table B1  
407  
408 R: Yes, same value is used for both species. This is a theoretical maximum for high water-content  
409 restrictions on photosynthesis (Frolking et al., 2002), which is needed but not our focus in the  
410 modelling.  
411  
412 L294 are listed  
413  
414 R: changed  
415  
416 L295-313 Why are snow dynamics important for the model?  
417  
418 R: Snow dynamics impact environmental conditions in the early growing season. As they are  
419 currently under change due to climate change, we considered important to include them for  
420 better predictions.  
421  
422 L318 What are “periodic lateral boundary conditions”?  
423  
424 R: rewritten  
425  
426 L323 of the model  
427  
428 R: added  
429  
430 L346-347 WTs is the multi-year mean of weekly water table?  
431  
432 R: clarified  
433  
434 L474 insert return  
435  
436 R: I was not able to find were to insert  
437  
438 L487 This would be a good place to explain why  $S_f$  overgrowsn  $S_m$  in the lawns.  
439

440 R: Explanation included. Basically, the looser structure of *S. fallax* allows its faster height growth.  
441  
442 L495 in other hydraulic  
443 R: added  
444  
445 L513 Explain the 0this could be because0, this is not obvious  
446  
447 R: the text was quite unclear, now clarified  
448  
449 L520 As Amax was lower in Sf, and Rs20 was the same, it seems that only Hspec would explain  
450 the result. You could repeat the test adjusting only Hspec to test this.  
451  
452 R: Hspec is a very powerful trait but our focus here was not to discuss each trait. Also, we don't  
453 have a species that would have lower in Hspec but resembles *S. fallax* in other traits. Therefore,  
454 we don't understand why this test would be meaningful.  
455  
456  
457 L527 dominated  
458  
459 R: modified  
460  
461 L544 This would be a good place to explain how these impacts work and what your model thus  
462 implies (or could imply when tested under climate-change conditions) for peatland stability and  
463 functioning  
464  
465 R: Explained  
466  
467 Table 1: I would recommend adding the units inside the table  
468  
469 R: added  
470  
471 Table 1 & Table B1: A in bryophytes is usually expressed in  $\text{nmol g}^{-1} \text{s}^{-1}$ , to avoid too many 0 before  
472 significant digits start.  
473  
474 R: we prefer to use the current version  
475  
476 Table 2 and 3: please explain abbreviations  
477  
478 R: explanation added  
479  
480 Appendix L 150 at one hertz?  
481  
482 R: Changed to every second.  
483

484 L209 The software is R, R Studio is just an interface

485

486 R: corrected

487

488 Fig B2: it is impossible to distinguish the models from the data especially in C. See comments

489 above about the curves in C.

490

491 R: The lines have now been redrawn. Fig B2 shows only measured values.

492 Referee 3

493

494 Major Comments

495

496 A. The Abstract and Introduction focus on feedbacks between the plant community structure and  
497 the environment. It seems from the outline of the model (Fig 1) and the descriptions of it that  
498 the environment serves as more of a forcing variable on the plant physiology and community  
499 dynamics. For example, there are no processes that feedback to the “Community environment”  
500 module in their model (Fig 1) and I did not see any not listed within the descriptions of the model  
501 structure in

502 the text. Clearly there are feedbacks between the capitula environment module and the shoot  
503 growth and competition module, but I don’t think the capitula environment is really what people  
504 would consider part of the plant’s environment. Fixing this will reframe the justification, but I  
505 think it can still be well justified.

506

507 R: The bold mentions on the feedback to hydrology in Abstract and Introduction are  
508 now removed as they were misleading.

509

510

511 B. In my opinion, the paper would be improved by applying the model to make predictions about  
512 a particular response to an environmental change. It could be argued that this paper is for model  
513 development and validation and the next one will use it in a predictive context. However, is there  
514 a small question that could be addressed with the model that would illustrate its value?

515

516 R: We agree that applying the model to predict change in community structure as  
517 a response to environmental change would be a logical next step and make the  
518 story far more interesting. However, as we are already here combining new  
519 empirical measurements conducted for model parameterizing and testing and  
520 description of the new model (and ending having a lot of text, tables and figures as  
521 appendix to keep the story readable) we see that adding more would be just too  
522 much.

523

524 C. I was surprised that the model did not deal with any of the autogenic processes that lead to  
525 hummock formation. The community model is spatially explicit and it would seem that it would  
526 allow for rule-based hummock formation simulation when succeeding from a high water table.  
527 Instead, the model simulates either high or low water tables. This seems like hummock forming  
528 processes would represent a true feedback to the environment. Is this either desirable or possible  
529 in this model iteration?

530

531 R: We agree that our model will be an excellent starting point to address autogenic  
532 processes that lead to hummock formation by including feedback to hydrology. We  
533 see PMS, the first model addressing Sphagnum community dynamics, as a  
534 steppingstone for the future work in numerical conceptualizing of peatland  
535 processes.

536 D. The living tissue of Sphagnum species clearly differ in their hydraulic conductivity (Km, p8; as  
537 shown in the McCarter and Price 2014 paper cited, see also Li, Glime and Liao 1992, J Bryology  
538 17:59); however, this was treated as a constant. Although I do not think there are reports of how  
539 this differs between *S. magellanicum* and *S. fallax*, I think it would be important to consider  
540 variation in this using hummock and hollow values for the two. I suspect that this would only  
541 accentuate the differences they observe in their results, and/or, speed up the time until species  
542 distributions equilibrate. In any case, given that species cover changes are quite sensitive to Km  
543 (Table 3), I think it is worth modeling species-specific differences in this parameter.

544  
545 R: We agree, but species-specific data on the hydraulic conductance was generally  
546 lacking. It would be very intriguing to see the impact of these parameters on  
547 modelling results, once the measurement date becomes available.  
548

549

550 Minor Comments

551  
552 E. I was surprised that the Titus and Wagner (1984, Ecology 65:1765) paper was not cited. Some  
553 of the simulation modeling is similar and should make for a nice comparison.  
554

555 R: Now included  
556

557

558 F. Need a table of abbreviations.

559  
560 R: Added  
561

562

563 G. It would be very helpful to show how the parameter values used fall within reported ranges in  
564 the literature (e.g., Table 1).

565  
566 R: We did a large search to fulfil this. Although we were able to find some  
567 meaningful values for comparison in the literature, we did not find them for most  
568 of the parameters and many of the ones related to photosynthesis were not  
569 measured in comparable conditions. For these reasons we abandoned the good  
570 idea to include ranges in the table but took the few ones found as subnotes in  
571 Table2 (previous Table 1).  
572

573

574 Specific Comments

575  
576 1. Line 81-2 Aren't they linked by capitulum water balance? Retention is too specific, I think.

577 R: modified

578

579

580 2. L101-4 I find this sentence confusing. Can you be more clear about the linkages?  
581 R: Rewritten to be clearer, as suggested by both reviewers.  
582

583 3. L142-3 I think it is controlled by water content  $\hat{A}$  Tnot the same thing as water retention.  
584 R: Rewritten  
585

586 4. Fig 1. What is the difference between dashed and solid lines? Can the boxes or arrows be  
587 changed so it is easier to tell that Module III influences Module II $\hat{A}$  Tit took a while to realize  
588 it wasn't controlled by precip and evap, where I thought the arrows were coming from. I would  
589 suggest making the figure legend more complete.  
590

591 R: In revised Fig 1, we added instructions to submodule boxes, replaced arrows from  
592 water balance to evaporation and capillary flow and added legend for different  
593 types of arrows in the figure.  
594

595 5. L213-18 This is the discussion of reseeded. It would be useful to know how frequently this was  
596 necessary. Was it rare with little impact on results or more common?  
597

598 R: The re-establishment from spore is calculated annually but it was not common  
599 in general. Most changes in grid cell occupants come from the invasion from  
600 neighboring cells. This process was mostly observed in the first two years of  
601 simulation, as the trait combination were randomly chosen, and consequently  
602 some combinations performed too poor to support the survival of individuals.  
603

604 6. L380-82 Is it worth listing what the parameters are meant here in text as is done below?  
605

606 R: We added list of symbols and abbreviations (New Table 1)  
607

608 7. Fig 2. The y-axis for the top figure should be "Relative Cover". Also, can you use solid and  
609 dashed lines to distinguish Hummock from Lawn? Would make it easier to read on B&W print.  
610 changed as suggested  
611

612 R: Modified as suggested  
613

614 8. L415 Why not show both species in both environments? Here only show *S. mag* in hummocks  
615 and *S. fal* in lawns.  
616 R: We have empirical data only from their natural habitats  
617

618 9. L418-23  
619 Would it be better to report these as elasticities (% change in outcome per % change  
620 in parameter). This is easy to do as they were all set to vary by +/- 10%. However, this  
621 would allow you to assess whether or not it was a large change or not $\hat{A}$   
622 Twhat would cutoff be? You report that being less than the standard deviation for a 10% change  
623 is

624 meaningful (L490), can you defend that?

625

626 R: We appreciate this suggestion and modified our statement

627

628 10. L469 You state that *S. fallax capitula* were less resistant to evaporation, but the data in Table  
629 B1 seem to indicate otherwise (see ra; this result is opposite to what I would expect although the  
630 do not differ significantly).

631

632 R: Rewritten to clarify. This was obviously unclearly expressed as it confused both  
633 reviewers.

634

635 11. L492 Yes, it would be expected for n to have a large effect as it is a scaling factor, so changes  
636 in its magnitude get amplified.

637

638 R: added to the text

639

640

641 12. L502-06 See Comment D above.

642

643 R: see response to D

644

645 13. L968 The procedure for doing the photosynthetic measurements would seem to cause quite  
646 a lot of drying within the cuvette (RH 60%, impeller at level 5) where they were measured over  
647 60-120 minutes. Were they rewetted following each light level? Were they allowed to dry? How  
648 did mass change during the course of the measurement and did that influence shape of curve?  
649 Can you provide a light response curve showing data? If there are not good answers to these  
650 questions, it would at least be helpful to include how the parameters measured compare with  
651 other ones in the literature.

652

653 R: We have added more details on the measurement protocol. The cuvette relative  
654 humidity was kept at 80% to slow down the drying process, but not to cause  
655 damage to the device.

656



657 Modelling the habitat preference of two key *Sphagnum* species in a poor fen as controlled by  
658 capitulum water retention

659 Jinnan Gong<sup>1</sup>, Nigel Roulet<sup>2</sup>, Steve Frolking<sup>1,3</sup>, Heli Peltola<sup>1</sup>, Anna M. Laine<sup>1,4</sup>, Nicola  
660 Kokkonen<sup>1</sup>, Eeva-Stiina Tuittila<sup>1</sup>

661 <sup>1</sup> School of Forest Sciences, University of Eastern Finland, P.O. Box 111, FI-80101 Joensuu,  
662 Finland

663 <sup>2</sup> Department of Geography, McGill University and Centre for Climate and Global Change  
664 Research, Burnside Hall, 805 rue Sherbrooke O., Montréal, Québec H3A 2K6

665 <sup>3</sup> Institute for the Study of Earth, Oceans, and Space, and Department of Earth Sciences,  
666 University of New Hampshire, Durham, NH 03824, USA

667 <sup>4</sup> Department of Ecology and Genetics, University of Oulu, P.O. Box 3000, FI-90014, Oulu,  
668 Finland

669

## 670 Abstract

671 Current peatland models generally lack dynamic ~~feedback-between-the~~ plant community structure  
672 ~~and-the-environment~~, although the vegetation dynamics and ecosystem functioning are tightly  
673 linked. Realistic projections of peatland response to climate change requires including vegetation  
674 dynamics in ecosystem models. In peatlands, *Sphagnum* mosses are key engineers. The ~~species~~  
675 ~~composition-in-a~~ moss community composition varies primarily ~~following~~ follows habitat  
676 moisture conditions. The species known preference along the prevailing moisture gradient might  
677 not directly serve as a reliable predictor for future species compositions as water table fluctuation  
678 is likely to increase. Hence, modelling the mechanisms ~~that~~ controlling the habitat preference  
679 of *Sphagna* is a good first step for modelling the community dynamics in peatlands. In this study,  
680 we developed the Peatland Moss Simulator (PMS), a process-based model, for simulating  
681 community dynamics of the peatland moss layer that results in habitat preferences of *Sphagnum*  
682 species along moisture gradients. PMS ~~employed~~ employs an individual-based approach to  
683 describe the variation of functional traits among shoots and the stochastic base of competition. At  
684 the shoot-level, growth and competition were driven by net photosynthesis, which was regulated  
685 by hydrological processes via capitulum water retention. The model was tested by predicting the  
686 habitat preferences of *S. magellanicum* and *S. fallax*, two key species representing dry (hummock)  
687 and wet (lawn) habitats in a poor fen peatland (Lakkasuo, Finland). PMS successfully captured the  
688 habitat preferences of the two *Sphagnum* species, based on observed variations in trait properties.  
689 Our model simulation further showed that the validity of PMS depended on the interspecific  
690 differences in capitulum water retention being correctly specified. Neglecting the water-retention  
691 differences led to the failure of PMS to predict the habitat preferences of the species in stochastic

692 simulations. Our work highlights the importance of capitulum water retention to the dynamics and  
693 carbon functioning of *Sphagnum* communities in peatland ecosystems. Studies of peatland  
694 responses to changing environmental conditions thus need to include capitulum water processes  
695 as a control on the vegetation dynamics. For that our PMS model could be used as an elemental  
696 design for the future development of dynamic vegetation models for peatland ecosystems.

697

698 **Keywords:** *Sphagnum* moss; capitulum water content; competition; peatland community  
699 dynamics; process-based modelling; moss traits; Peatland Moss Simulator (PMS)

700

## 701 1.Introduction

702 Peatlands have important roles in the global carbon cycle as they store about 30% of the world's  
703 soil carbon (Gorham, 1991; Hugelius et al., 2013). Environmental changes, like climate warming  
704 and land-use changes, are expected to impact the carbon functioning of peatland ecosystems  
705 (Tahvanainen, 2011). Predicting the functioning of peatlands under environmental changes  
706 requires models to quantify the interactions among ecohydrological, ecophysiological and  
707 biogeochemical processes. These processes are known to be strongly regulated by vegetation  
708 (Riutta et al. 2007; Wu and Roulet, 2014), which can change during decadal timeframe under  
709 changing hydrological conditions (Tahvanainen, 2011). Current peatland models generally lack  
710 mechanisms for the dynamical ~~feedbacks between vegetation-plant community structure and~~  
711 ~~environment~~ (e.g. Frohking et al., 2002; Wania et al., 2009). Therefore, those ~~feedback~~ mechanisms  
712 need to be identified and integrated with ecosystem processes, in order to support realistic  
713 predictions on peatland functioning and the research community working on global  
714 biogeochemical cycles.

715 A major fraction of peatland biomass is formed by *Sphagnum* mosses (Hayward and Clymo,  
716 1983; Vitt, 2000). Although individual *Sphagnum* species often ~~has~~have narrow habitat niches  
717 (Johnson et al., 2015), different *Sphagnum* species replace each other along water -table gradient  
718 and therefore, as a genus, spread across a wide range of water table conditions ([Rydin and](#)  
719 [McDonald, 1985](#); Andrus et al. 1986; [Rydin, 1993](#); Laine et al. 2009; ~~Rydin and McDonald, 1985~~).  
720 The species composition of the *Sphagnum* community strongly affects ecosystem processes such  
721 as ~~hydrology~~, carbon sequestration and peat formation through interspecific variability in species  
722 traits such as photosynthetic potential and litter quality (Clymo, 1970; O'Neill, 2000; Vitt, 2000;  
723 Turetsky, 2003). The production of biomass and litter from *Sphagna*, which gradually raises the  
724 moss carpet, in turn affects the species composition (Robroek et al. 2009). Hence, modelling the  
725 moss community dynamics is fundamental for predicting temporal changes of peatland vegetation.  
726 As the distribution of *Sphagnum* species primarily follows the variability in water level-table in a  
727 peatland ~~community~~ (Andrus 1986; Väiliranta et al. 2007), modelling the habitat preference of

728 *Sphagnum* species along a moisture gradient could be a good first step for predicting moss  
729 community dynamics in peatland ecosystems, ~~based on “space for time” substitution~~ (Blois et al.,  
730 2013).

731 For a given *Sphagnum* species, the ~~preferable~~-optimal habitat represents the environmental  
732 conditions for it to achieve higher rates of net photosynthesis and shoot elongation than the peers  
733 ([Titus & Wagner, 1984](#); [Rydin & McDonald, 1985](#); [Rydin, 1997](#); Robroek et al., 2007a; Keuper  
734 et al., 2011). Capitulum water content, which is determined by the balance between the evaporative  
735 loss and water gains from capillary rise and precipitation, represents one of the most important  
736 controls on net photosynthesis ([Titus & Wagner, 1984](#); Murray et al. 1989; Van Gaalen et al. 2007;  
737 Robroek et al., 2009). To quantify the water processes in mosses, hydrological models have been  
738 developed to simulate the water movement between moss carpet and the peat underneath (Price,  
739 2008; Price and Waddington, 2010), as regulated by the variations in meteorological conditions  
740 and energy balance. On the other hand, experimental work has addressed the species-specific  
741 responses of net photosynthesis to changes in capitulum water content ([Titus & Wagner, 1984](#);  
742 Hájek and Beckett, 2008; Schipperges and Rydin, 2009) and light intensity (Rice et al., 2008;  
743 Laine et al., 2011; Bengtsson et al., 2016). Net photosynthesis and hydrological processes are  
744 linked via capitulum water retention, which controls the response of capitulum water content to  
745 water potential changes (Jassey & Signarbieux, 2019). However, these mechanisms have not been  
746 integrated with ecosystem processes in modelling. Due to the lack of quantitative tools, the  
747 hypothetical importance of capitulum water retention has not yet been verified.

748 Along with ~~the need for quantifying~~ the capitulum water processes, modelling the habitat  
749 preference of *Sphagna* ~~requires needs to quantify quantification of~~ the competition among mosses,  
750 ~~which is referred to as i.e.~~, the “race for space” ([Rydin, 1993](#); [Rydin, 1997](#); Robroek et al., 2007a;  
751 Keuper et al., 2011): *Sphagnum* shoots could form new capitula and spread laterally, if there is  
752 space available. This reduces or eliminates the light source for any plant that ~~being is covered~~  
753 ~~buried by peers underneath~~ (Robroek et al. 2009). As the competition occur between neighboring  
754 shoots, its modelling requires downscaling water-energy processes from the ecosystem to the shoot  
755 level. For that, *Sphagnum* competition needs to be modelled as spatial processes, considering that  
756 spatial coexistence and the variations of functional traits among shoot individuals may impact the  
757 community dynamics (Bolker et al., 2003; Amarasekare, 2003). However, ~~existing ? coexistence~~  
758 generally rely on simple coefficients to describe the interactions among individuals (e.g. Czárán  
759 and Iwasa, 1998; Anderson and Neuhauser, 2000; Gassmann et al., 2003; Boulangeat et al., 2018),  
760 thus being decoupled from environmental fluctuation or the stochasticity of biophysiological  
761 processes.

762 This study aims to develop and test a model, the Peatland Moss Simulator (PMS), to simulate  
763 community dynamics within the peatland moss layer that results in realistic habitat preference of  
764 *Sphagnum* species along a moisture gradient. In PMS, community dynamics is driven by

765 *Sphagnum* photosynthesis. ~~is the central process driving community dynamics~~ Photosynthesis in  
766 ~~turn is regulated and its competitiveness in the environment is controlled by~~ capitulum water  
767 ~~retention through the~~ capitulum moisture content. ~~The moisture content in turn is controlled by~~  
768 ~~capitulum water retention and water balance~~. Therefore, we hypothesize that water retention of the  
769 capitula is the mechanism driving moss community dynamics. We test the model validity using  
770 data from an experiment based on two *Sphagnum* species with different positions along moisture  
771 gradient in the same peatland site. If our hypothesis holds, the model will (1) correctly predict the  
772 competitiveness of the two species in wet and dry habitats; and (2) fail to predict competitiveness  
773 if the capitulum water retention of the two species are not correctly specified.

774

## 775 2. Materials and methods

### 776 2.1 Study site

777 The peatland site being modelled locates in Lakkasuo, Orivesi, Finland (61° 47' N; 24° 18' E).  
778 The site is a poor fen fed by mineral inflows from a nearby esker (Laine et al 2004). Most of the  
779 site is formed by lawns dominated by *Sphagnum recurvum* complex (*Sphagnum fallax*,  
780 accompanied by *Sphagnum flexuosum* and *Sphagnum angustifolium*) and *Sphagnum papillosum*.  
781 Less than 10% of surface are occupied by hummocks, which are 15-25 cm higher than the lawn  
782 surface with *Sphagnum magellanicum* and *Sphagnum fuscum*. Both microforms are covered by  
783 continuous *Sphagnum* carpet with a sparse ~~cover of ground~~-vascular ~~canopies plants~~ (projection  
784 cover of *Carex* 12% on average), which spread homogeneously over the topography. The annual  
785 mean water table was  $15.6 \pm 5.0$  cm deep from lawn surface (Kokkonen et al., 2019). More  
786 information about the site can be found in Kokkonen et al. (2019).

787

### 788 2.2 Model outline

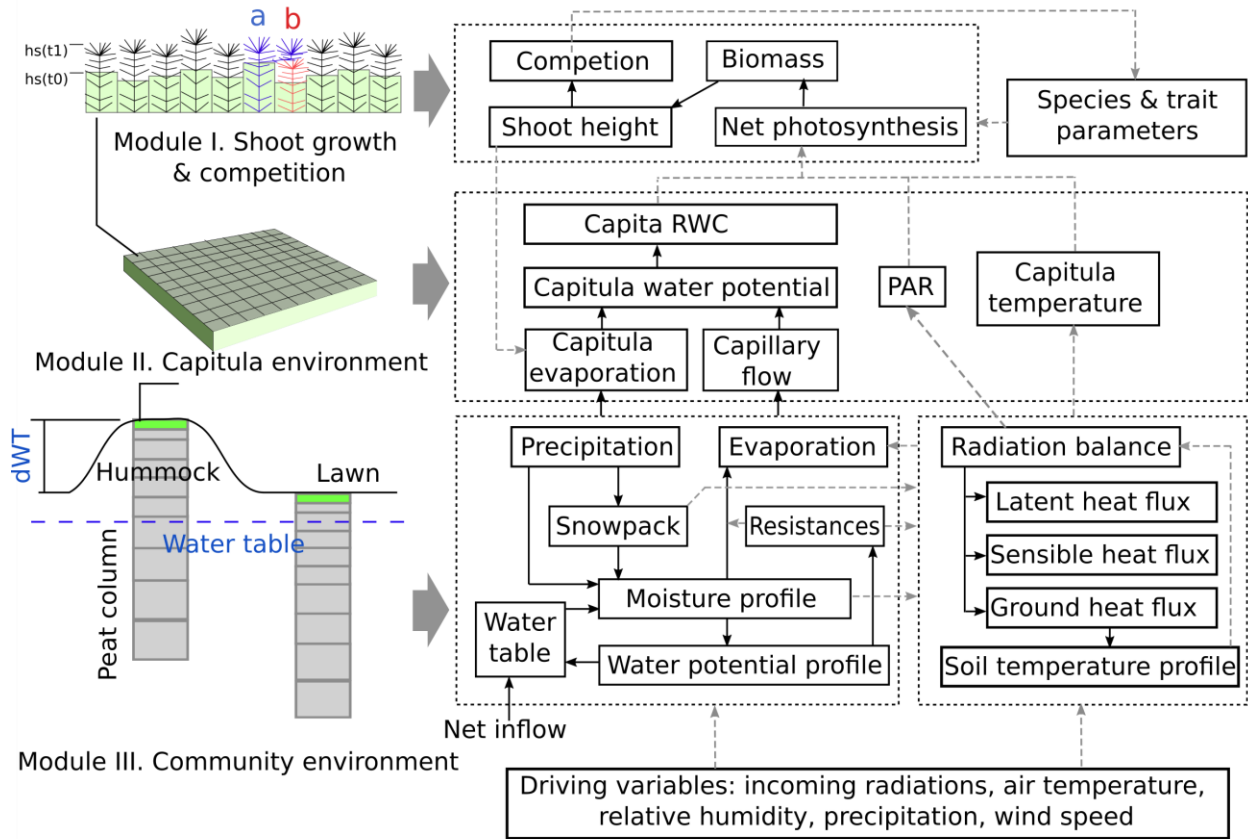
789 The Peatland Moss Simulator (PMS) is a process-based, stochastic model, which simulates the  
790 temporal dynamics of *Sphagnum* community as driven by variations in precipitation, irradiation,  
791 and energy flow ~~water-energy conditions~~ and individual-based interactions (Fig. 1). In PMS, the  
792 studied ecosystem is seen as a dual-column system consisting of hydrologically connected  
793 habitats of hummocks and lawns (community environment in Fig. 1). For each habitat type, the  
794 community area is downscaled to two-dimensional cells representing the scale of individual shoots  
795 (i.e. 1 cm<sup>2</sup>). Each grid cell can be occupied by one capitulum from a single *Sphagnum* species. The  
796 community dynamics, i.e. the changes in species abundances, ~~were~~ are driven by the growth and  
797 competition of *Sphagnum* shoots at the grid-cell level (Module I in Fig. 1). These processes were  
798 regulated by the grid-cell-specific conditions of water and energy (Module II in Fig. 1), which are  
799 derived from the community environment (Module III in Fig. 1).

800 In this study, we focused on developing Module I and II (Section 2.3) and employed an available  
801 soil-vegetation-atmosphere transport (SVAT) model (Gong et al., 2013a, 2016) to describe the  
802 water-energy processes for Module III (Appendix A). We assumed that the temporal variation in  
803 water-table was similar in lawns and hummocks, and the hummock-lawn differences in water  
804 table ( $dWT$  in Fig. 1) followed their difference in surface elevations (Wilson, 2012). At the grid  
805 cell level, the photosynthesis of capitula drove the biomass growth and elongation of shoots, which  
806 led to the “race for space” between adjacent grid cells. The net photosynthesis rate was controlled  
807 by capitulum water content ( $W_{cap}$ )~~capitulum water retention~~, which ~~was defines~~ defined by the  
808 capitulum water retention in relation responses of capitulum water content ( $W_{cap}$ ) to water potential  
809 ( $h$ ) ~~changes~~ (Section 2.4). The values for functional traits that regulating regulate the growth and  
810 competition processes were ~~considered as~~ randomly selected within their normal distribution  
811 measured in the field variables (Section 2.4). Unknown parameters that related the lateral water  
812 flows of the site are estimated using a machine-learning approach (Section 2.5). Finally, Monte-  
813 Carlo simulation was used to support the analysis on the habitat preferences of *Sphagnum* species  
814 and hypothesis tests (Section 2.6). The list of used symbols is given in Table 1.

815

816

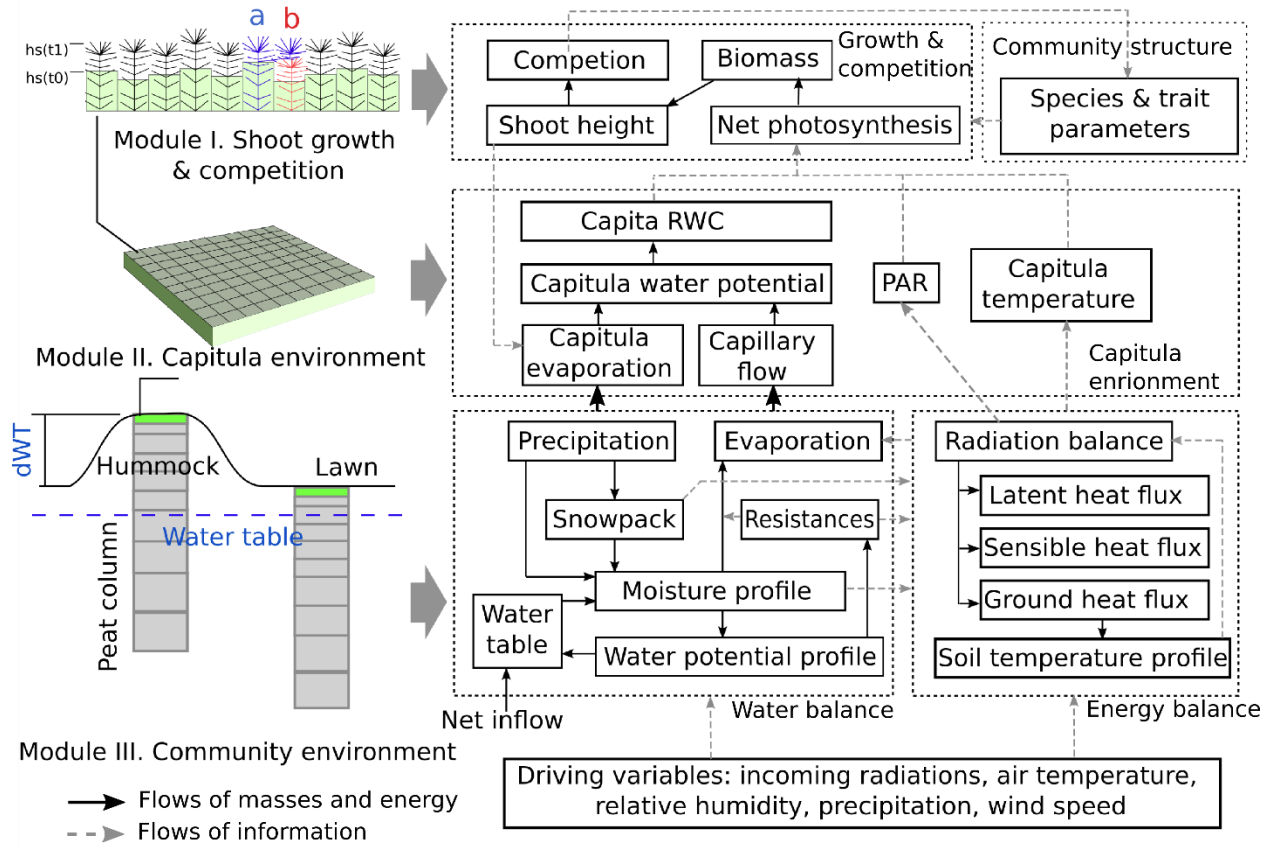
817



818

819





820

821 Fig. 1 Framework of Peatland Moss Simulator (PMS).

822

## 823 2.3 Model development

### 824 2.3.1 Calculating shoot growth and competition of Sphagnum mosses (Module I)

#### 825 Calculation of Sphagnum growth

826 To model grid cell biomass production and height increment, we assumed that capitula were the  
 827 main parts of shoots responsible for photosynthesis and production of new tissues, instead of the  
 828 stem sections underneath. We employed a hyperbolic light-saturation function (Larcher, 2003) to  
 829 calculate the net photosynthesis, which was parameterized based on empirical measurements made  
 830 from the target species collected from the study site (see Appendix B for materials and methods):

$$831 A_{20} = \left( \frac{Pm_{20} * PPF D}{\alpha_{PPFD} + PPF D} - R_{S_{20}} \right) * B_{cap} \quad (1)$$

832 where subscript 20 denotes the variable value measured at 20 °C;  $R_s$  is the mass-based respiration  
 833 rate ( $\mu\text{mol g}^{-1} \text{s}^{-1}$ );  $Pm$  is the mass-based rate of maximal gross photosynthesis ( $\mu\text{mol g}^{-1} \text{s}^{-1}$ );  $PPFD$   
 834 is the photosynthetic photon flux density ( $\mu\text{mol m}^{-2} \text{s}^{-1}$ ); and  $\alpha_{PPFD}$  is the half-saturation point  
 835 ( $\mu\text{mol m}^{-2} \text{s}^{-1}$ ) for photosynthesis.

836 By adding multipliers for capitula water content ( $f_W$ ) and temperature ( $f_T$ ) to Eq. (1), the net  
837 photosynthesis rate  $A$  ( $\mu\text{mol m}^{-2} \text{s}^{-1}$ ) was calculated as following:

$$838 \quad A = \left[ \frac{Pm_{20} * PPFD}{\alpha_{PPFD} + PPFD} f_T(T) - R_{s20} f_R(T) \right] * B_{cap} * f_W(W_{cap}) \quad (2)$$

839 where  $f_W(W_{cap})$  describes the responses of  $A$  to capitulum water content,  $W_{cap}$ ;  $f_T(T)$  describes  
840 the responses of  $Pm$  to capitulum temperature  $T$  (Korrensalo et al., 2017).  $f_W(W_{cap})$  was estimated  
841 based on the empirical measurements (Appendix B; see Section 2.4). The temperature response  
842  $f_R(T)$  is a  $Q_{10}$  function that describes the temperature sensitivity of  $R_s$  (Frolking et al., 2002):

$$843 \quad f_R(T) = Q_{10}^{(T-T_{opt})/10} \quad (3)$$

844 where  $Q_{10}$  is the sensitivity coefficient;  $T$  is the capitulum temperature ( $^{\circ}\text{C}$ );  $T_{opt}$  ( $20^{\circ}\text{C}$ ) is the  
845 reference temperature of respiration.

846 The response of  $A$  to  $W_{cap}$  ( $f_W(W_{cap})$ , Eq. 2) was described as a second-order polynomial function  
847 (Gong et al., 2019):

$$848 \quad f_W(W_{cap}) = a_{W0} + a_{W1} * W_{cap} + a_{W2} * W_{cap}^2 \quad (4)$$

849 where  $a_{W0}$ ,  $a_{W1}$  and  $a_{W2}$  are coefficients.

850 Plants can store carbohydrates as nonstructural carbon (NSC, e.g. starch and soluble sugar) to  
851 support fast growth in spring or post-stress periods, like after drought events (Smirnoff et al., 1992;  
852 Martínez-Vilalta et al., 2016; Hartmann and Trumbore, 2016). We linked the production of shoot  
853 biomass to the immobilization of NSC storage (modified from Eq. 10 in Asaeda and Karunaratne,  
854 2000). The change in NSC storage depends on the balance between net photosynthesis and  
855 immobilization:

$$856 \quad M_B = s_{imm} * NSC * k_{imm} \alpha_{imm}^{T-20} \quad (5)$$

$$857 \quad \partial NSC / \partial t = A - M_B, NSC \in [0, NSC_{max}] \quad (6)$$

858 where  $M_B$  is the immobilized NSC to biomass production during a time step (g);  $k_{imm}$  is the specific  
859 immobilization rate ( $\text{g g}^{-1}$ ) (Asaeda and Karunaratne 2000);  $\alpha_{imm}$  is the temperature constant;  $s_{imm}$   
860 is the multiplier for temperature threshold, where  $s_{imm} = 1$  when  $T > 5^{\circ}\text{C}$  but  $s_{imm} = 0$  if  $T \leq 5^{\circ}\text{C}$ .  
861  $NSC_{max}$  is the maximal NSC concentration in *Sphagnum* biomass (Turetsky et al., 2008). Timing  
862 of growth is controlled by a temperature threshold and NSC availability. Growth occurs when  $T >$   
863  $5^{\circ}\text{C}$  and NSC is above zero. The dynamics of NSC storage are related to WC through net  
864 photosynthesis.

865 The increase in shoot biomass drove the shoot elongation:

$$866 \quad \partial H_c / \partial t = \frac{M_B}{H_{spc} S_c} \quad (7)$$



867 where  $H_c$  is the shoot height (cm);  $H_{spc}$  is the biomass density of *Sphagnum* stems ( $\text{g m}^{-2} \text{cm}^{-1}$ ) and  
868  $S_c$  is the area of a cell ( $\text{m}^2$ ).

869

### 870 *Calculation of Sphagnum competition and community dynamics*

871 To simulate the competition among *Sphagnum* shoots, we first compared  $H_c$  of each grid cell  
872 (source grid cell, i.e. grid cell  $a$  in Fig. 1) to its four neighboring cells and marked the one with  
873 lowest position (e.g. grid cell  $b$  in Fig. 1) as the target of spreading. The spreading of shoots from  
874 a source to a target grid cell occurred when the following criteria were fulfilled: i) the height  
875 difference between source and target grid cells exceeded a threshold value; ii) ~~NSC~~~~the biomass~~  
876 accumulation in the source grid cell was large enough to support the growth of new capitula in the  
877 target grid cell; iii) the capitula in the source grid cell can split at most once per year.

878 The threshold of height difference in rule i) was set equal to the mean diameter of capitula in  
879 the source cell, based on the assumption that the shape of a capitulum was spherical. When shoots  
880 spread, the species type and model parameters in the target grid cell were overwritten by those in  
881 the source grid cell, assuming the mortality of shoots originally in the target cell. During the  
882 spreading, ~~biomass and NSC storage were was~~ transferred from the source cell to the target cell to  
883 form new capitula. ~~In case that the NSC storage in grid cell was exhausted, the metabolism of~~  
884 ~~shoots became deactivated and the biomass growth or spreading stopped immediately. Sphagnum~~  
885 ~~shoots in these deactivated grid cells could be re-established by invasion from neighboring cells.~~  
886 In cases where spreading did not take place, establishment of new shoots from spores was allowed  
887 to maintain the continuity of *Sphagnum* carpet at the site. During the establishment from spores,  
888 ~~which was rare and occurred during the first years of simulation,~~ the ~~type properties~~ of *Sphagnum*  
889 species ~~was were~~ randomized ~~within their normal distribution measured in the field with moss~~  
890 ~~parameters initialized as random numbers based on the measured means and variations.~~

891

### 892 **2.3.2 Calculating grid cell-level dynamics of environmental factors (Module II)**

893 Module II computes grid-cell values of  $W_{cap}$ ,  $PPFD$  and  $T$  for Module I. The cell-level  $PPFD$  and  
894  $T$  were assumed to be equal to the community means, which were solved by the SVAT scheme in  
895 Module III (Appendix A.). The community level evaporation rate ( $E$ ) was partitioned to cell-level  
896 ( $E_i$ ) as following:

$$897 \quad E_i = E * \left( \frac{Sv_i}{r_{bulk,i}} \right) / \sum \left( \frac{Sv_i}{r_{bulk,i}} \right) \quad (8)$$

898 where  $r_{bulk,i}$  is the bulk surface resistance of cell  $i$ , which is as a function ( $r_{bulk,i} = fr(h_i)$ ) of grid-  
899 cell-based water potential  $h_i$ , capitulum biomass ( $B_{cap}$ ) and shoot density ( $D_S$ ) based on the  
900 empirical measurements (Appendix B);  $Sv_i$  was the evaporative area, which was related to the

901 height differences among adjacent grid cells:

$$902 \quad Sv_i = Sc_i + lc \sum_j (Hc_i - Hc_j) \quad (9)$$

903 where  $lc$  is the width of a grid cell (cm); and subscript  $j$  denotes the four-nearest neighbouring grid  
904 cells. In this way, changes in the height difference between the neighboring shoots feeds back to  
905 affect the water conditions of the grid cells, via alteration of the evaporative surface area.

906 The grid cell-level changes in capitula water potential ( $h_i$ ) was driven by the balance between  
907 the evaporation ( $E_i$ ) and the upward capillary flow ~~from the center of moss layer~~ to capitula:

$$908 \quad \partial h_i = \frac{K_m}{C_i} \left[ \frac{(h_i - h_m)}{0.5z_m} - 1 - E_i \right] \quad (10)$$

909 where  $h_m$  is the water potential of the living moss layer, solved in Module III (Appendix A.);  $z_m$  is  
910 the thickness of the living moss layer ( $z_m=5$  cm);  $K_m$  is the hydraulic conductivity of the moss layer  
911 and that is set to be the same for each grid cell;  $C_i$  is the cell-level specific ~~capacity of water uptake~~  
912 capacity ( $C_i = \partial W_{cap,i} / \partial h_i$ ).  $\partial W_{cap,i} / \partial h_i$  could be derived from the capitulum water retention function  
913  $h_i = f_h(W_{cap})$ .  $W_{cap}$  can be then calculated from the estimated from  $h_i$  and affect the calculation of  
914 net photosynthesis through  $f_w(W_{cap})$  (Eq. 2).

915

## 916 **2.4 Model parameterization**

### 917 *Selection of Sphagnum species*

918 We chose *S. fallax* and *S. magellanicum*, which form 63% of total plant cover at the study site at  
919 Lakkasuo (Kokkonen et al., 2019), as the target species representing the lawn and hummock  
920 habitats respectively. These species share similar a niche along the gradients of soil pH and nutrient  
921 richness (Wojtuń et al., 2003), but are discriminated by their preferences of water-table level  
922 (Laine et al., 2004). While *S. fallax* is commonly found close to the water table (Wojtuń et al.,  
923 2003), *S. magellanicum* can occur along a wider range of a dry-wet gradient, from intermediately  
924 wet lawns up to dry hummocks (Rice et al., 2008; Kyrkjeeide, et al., 2016; Korresalo et al., 2017).  
925 The transition from *S. fallax* to *S. magellanicum* along the wet-dry gradient thus indicates the  
926 decreasing competitiveness of *S. fallax* against *S. magellanicum* with a lowering water table.

### 927 *Parameterization of morphological traits, net photosynthesis and capitulum water retention*

928 We empirically quantified the morphological traits capitulum density ( $D_s$ , shoots  $\text{cm}^{-2}$ ), biomass  
929 of capitula ( $B_{cap}$ ,  $\text{g m}^{-2}$ ), biomass density of living stems ( $H_{spc}$ ,  $\text{g cm}^{-1} \text{m}^{-2}$ ), net photosynthesis  
930 parameters ( $Pm_{20}$ ,  $RS_{20}$  and  $\alpha_{PPFD}$ ) and the water retention properties (i.e.,  $f_h(W_{cap})$  and  $fr(h)$ , Eqs.  
931 8 and 10) for the selected species from the same site (see Appendix B for methods). The values  
932 (mean  $\pm$  SD) of the morphological parameters, the photosynthetic parameters and polynomial  
933 coefficients ( $a_{w0}$ ,  $a_{w1}$  and  $a_{w2}$ , Eq. 3) are listed in Table: ~~12~~. For each parameter, a random value

934 was initialized for each cell based on the measured means and SD, assuming the variation of  
935 parameter values is normally distributed.

936 We noticed that the fitted  $f_W(W_{cap})$  was meaningful when  $W_{cap} < W_{opt}$ , ~~which is~~ was below the  
937 optimal water content for photosynthesis ( $W_{opt} = -0.5 a_{W1}/ a_{W2}$ ). If  $W_{cap} > W_{opt}$ , photosynthesis  
938 decreased linearly with increasing  $W_{cap}$ , as being limited by the diffusion of CO<sub>2</sub> (Schipperges and  
939 Rydin, 1998). In that case,  $f_W(W_{cap})$  was calculated following Frohking et al. (2002):

$$940 \quad f_W(W_{cap}) = 1 - 0.5 \frac{W_{cap} - W_{opt}}{W_{max} - W_{opt}} \quad (11)$$

941 where  $W_{max}$  is the maximum water content of capitula.

942 It is known that  $W_{max}$  is around 25-30 g g<sup>-1</sup> (e.g. Schipperges and Rydin, 1998), or about 0.31 -  
943 0.37 cm<sup>3</sup> cm<sup>-3</sup> in term of volumetric water content (assuming 75 g m<sup>-2</sup> capitula biomass and 0.6  
944 cm height of capitula layer). This range is broadly lower than the saturated water content of moss  
945 carpet (> 0.9 cm<sup>3</sup> cm<sup>-3</sup>, McCarter and Price, 2014). Consequently, we used the following equation  
946 to convert volumetric water content to capitula RWC, when  $h_i$  was higher than the boundary value  
947 of -10<sup>4</sup> cm:

$$948 \quad W_{cap} = \min(W_{max}, \theta_m / (H_{cap} * B_{cap} * 10^{-4})) \quad (12)$$

949 where  $W_{max}$  is the maximum water content that set to 25 g g<sup>-1</sup> for both species;  $\theta_m$  is the volumetric  
950 water content of moss layer;  $H_{cap}$  is the height of capitula and is set to 0.6 cm (Hájek and Beckett,  
951 2008).

## 952 *Parameterization of SVAT processes*

953 For the calculation of surface energy balance, we set the height and leaf area of vascular canopy  
954 to 0.4 m and 0.1 m<sup>2</sup> m<sup>-2</sup>, consistent with the scarcity of vascular canopies at the site. The  
955 aerodynamic resistance ( $r_{aero}$ , Eq. A14, Appendix A) for surface energy fluxes was calculated  
956 following Gong et al. (2013a). The bulk surface resistance of community ( $r_{ss}$ , Eq. A13, Appendix  
957 A) was summarized from the cell-level values of  $r_{bulk,i}$ , that  $1/r_{ss} = \sum(1/r_{bulk,i})$ . To calculate the  
958 peat hydrology and water table, peat profiles of hummock and lawn communities were set to 150  
959 cm deep and stratified into horizontal layers of depths varying from 5cm (topmost) to 30cm  
960 (deepest). For each peat layer, the thermal conductivity ( $K_T$ ) of fractional components, i.e. peat,  
961 water and ice, were evaluated following Gong et al. (2013a). The bulk density of peat ( $\rho_{bulk}$ ) was  
962 set to 0.06 g cm<sup>-3</sup> below acrotelm (40 cm depth, Laine et al., 2004), and decreased linearly toward  
963 the living moss layer. The saturated hydraulic conductivity ( $K_{sat}$ , Eq. A6, Appendix A) and water  
964 retention parameters (i.e.  $\alpha$  and  $n$ , Eq. A5, Appendix A) of water retention curves were calculated  
965 as functions of  $\rho_{bulk}$  and the depth of peat layer following Päivänen (1973).  $K_{sat}$ ,  $\alpha$  and  $n$  for the  
966 living moss layer were adopted from the values measured by McCarter and Price (2014) from *S.*  
967 *magellanicum* carpet. The parameter values for SVAT processes ~~were~~ are listed in Table. [23](#).

969 [In boreal and arctic regions, the amount and timing of snow melt has crucial impact on moisture](#)  
 970 [conditions, especially at fen peatlands. Therefore, ~~To have realistic spring conditions in the~~](#)  
 971 [beginning of the growing season](#) ~~We we~~ introduced a snow-pack model, SURFEX v7.2 (Vionnet  
 972 et al., 2007), into the SVAT modelling. The snow-pack model simulates snow accumulation, wind  
 973 drifting, compaction and changes in metamorphism and density. These processes influenced the  
 974 heat transport and freezing-melting processes (i.e.  $S_h$  and  $S_T$ , see Eq. A1-A2, Appendix A). In this  
 975 modelling, we calculate the snow dynamics on a daily basis in parallel to the SVAT simulation.  
 976 Daily snowfall was converted into a snow layer and added to ground surface. For each of the day-  
 977 based snow layers (D-layers), we calculated the changes in snow density, particle morphology and  
 978 layer thicknesses. At each time step, D-layers were binned into layers of 5-10 cm depths (S-layers)  
 979 and placed on top of the peat column for SVAT modelling. With a snow layer present, surface  
 980 albedos (i.e.  $a_s$ ,  $a_l$ ) were modified to match those of the topmost snow layer (see Table- 4 in Vionnet  
 981 et al., 2007). If the total thickness of snow was less than 5 cm, all D-layers were binned into one  
 982 S-layer. The thermal conductivity ( $K_T$ ), specific heat ( $C_T$ ), snow density, thickness and water  
 983 content of each S-layer were calculated as the mass-weighted means from the values of D-layers.  
 984 Melting and refreezing tended to increase the density and  $K_T$  of a snow layer but decrease its  
 985 thickness (see Eq. 18 in Vionnet et al., 2007). The fraction of melted water that exceeded the water  
 986 holding capacity of a D-layer (see Eq. 19 in Vionnet et al., 2007) was removed immediately as  
 987 infiltration water. If the peat layer underneath was saturated, the infiltration water was removed  
 988 from the system as lateral discharge.

### 989 *Boundary conditions and driving variables*

990 A zero-flow boundary was set at the bottom of peat ~~columns~~. [At peat surface](#) ~~The the~~ boundary  
 991 conditions of water and energy ~~at peat surface~~ were defined by the ground surface temperature ( $T_0$ ,  
 992 see Eq. A10-A15 in Appendix A) and the net precipitation ( $P$  minus  $E$ ). The profiles of layer  
 993 thicknesses,  $\rho_{bulk}$  and hydraulic parameters were assumed to be constant during simulation.  
 994 ~~Periodic~~ ~~H~~ lateral boundary conditions were used to calculate the spreading of *Sphagnum* shoots  
 995 among cells along the edge of the model domain [so that shoots can spread across the edge of](#)  
 996 [simulation area and invade into the grid cell at the boarder of the opposite side](#).

997 The model simulation was driven by climatic variables of air temperature ( $T_a$ ), precipitation  
 998 ( $P$ ), relative humidity ( $Rh$ ), wind speed ( $u$ ), incoming shortwave radiation ( $R_s$ ) and longwave  
 999 radiation ( $R_l$ ). To support the stochastic parameterization of [the](#) model and Monte-Carlo  
 1000 simulations, Weather Generator (Strandman et al., 1993) was used to generate randomized  
 1001 scenarios based on long-term weather statistics (period of 1981-2010) from 4 closest weather  
 1002 stations of Finnish Meteorological Institute. This generator had been intensively tested and applied  
 1003 under Finnish conditions (Kellomäki and Väisänen, 1997; Venäläinen et al., 2001; Alm et al.,  
 1004 2007). We also compared the simulated meteorological variables against 2-year data measured

1005 from Siikaneva peatland site (61°50 N; 24°10 E), located 10 km away from our study site  
1006 (Appendix C).

1007

## 1008 **2.5 Model calibration for lateral water influence**

1009 We used a machine-learning approach to estimate the influence of upstream area on the water  
1010 balance of the site. The rate of net inflow ( $I$ , see Eq. A18 in Appendix A.) was described as a  
1011 function of Julian day ( $JD$ ), assuming the inflow was maximum after spring thawing and then  
1012 decreased linearly with time:

$$1013 I_j = (a_N * JD + b_N) * Ks_j, JD > JD_{thaw} \quad (11)$$

1014 where subscript  $j$  denotes the peat layers under water table;  $Ks$  is the saturated hydraulic  
1015 conductivity;  $JD_{thaw}$  is the Julian day that thawing completed; and  $a_N$  and  $b_N$  are parameters.

1016 We simulated water table changes using climatic scenarios from the Weather Generator (Section  
1017 2.4). During the calibration, the community compositions were set constant, that *S. magellanicum*  
1018 fully occupied the hummock habitat whereas *S. fallax* fully occupied the lawn habitat. The  
1019 simulated multi-year means of weekly water table values were compared to the weekly mean water  
1020 table obtained observed at the site during years 2001, 2002, 2004 and 2016. The cost function for  
1021 the learning process was based on the sum of squared error ( $SE$ ) of the simulated water table:

$$1022 SE = \Sigma(WTs_k - Wtm_k)^2 \quad (12)$$

1023 where  $Wtm$  is the measured multi-year weekly mean of water table;  $WTs$  is the simulated multi-  
1024 year weekly mean of water table; and subscript  $k$  denotes the week of year when the water table  
1025 was sampled.

1026 The values of  $a_N$  and  $b_N$  were estimated using the Gradient Descent approach (Ruder, 2016), by  
1027 minimizing  $SE$  in above Eq. (19):

$$1028 X_N(j) := X_N(j) - \Gamma \frac{\partial SE}{\partial X_N(j)} \quad (13)$$

1029 where  $\Gamma$  is the learning rate ( $\Gamma = 0.1$ ). Appendix D shows the simulated water table with the  
1030 calibrated inflow term  $I$ , as compared against the measured values from the site.

1031

## 1032 **2.6 Model-based analysis**

1033 First, we examined the ability of model to capture the preference of *S. magellanicum* for the  
1034 hummock environment and *S. fallax* for the lawn environment (Test 1). For both species, the  
1035 probability of occupation was initialized as 50% in a cell, and the distribution of species in the  
1036 communities were randomly patterned. Monte-Carlo simulations (40 replicates) were carried out,

1037 with a time step of 30 minutes. A simulation length of 15 years was selected based on preliminary  
1038 studies, in order to cover the major part of change and ease the computational demand. Biomass  
1039 growth, stem elongation and the spreading of shoots were simulated on a daily basis. The  
1040 establishment of new shoots in deactivated cells was calculated at the end of each simulation year.  
1041 We then assessed if the model could capture the dominance of *S. magellanicum* in the hummock  
1042 communities and the dominance of *S. fallax* in lawn communities. The simulated annual height  
1043 increments of mosses were compared to the values measured for each community type. To measure  
1044 moss height growth, we deployed 20 cranked wires on *S. magellanicum* dominated hummocks and  
1045 15 on *S. fallax* dominated lawns in 2016. Each cranked wire was a piece of metal wire attached  
1046 with plastic brushes at the side anchored into the moss carpet (e.g. Clymo 1970, Holmgren et al.,  
1047 2015). Annual height growth ( $dH$ ) was determined by measuring the change in the exposed wire  
1048 length above moss surface from the beginning to the end of growing season.

1049 Second, we tested the robustness of the model to the uncertainties in a set of parameters (Test  
1050 2). We focused on parameters that closely linked to hydrology and growth calculations, but were  
1051 roughly parameterized (e.g.  $k_{imm}$ ,  $r_{aero}$ ) or adopted as a prior from other studies (e.g.  $K_{sat}$ ,  $\alpha$ ,  $n$ ,  
1052  $NSC_{max}$ ; see Table 23). One at a time, each parameter value was adjusted by +10 % or -10 %, and  
1053 species cover was simulated using the same runtime settings as Test 1 with 40 Monte-Carlo runs.  
1054 The simulated means of cover were then compared to those calculated without the parameter  
1055 adjustment.

1056 Tests 3-4 were then carried out to test whether the model could correctly predict competitiveness  
1057 of the species in dry and wet habitats, if the species-specific trends of capitulum water retention  
1058 were not correctly specified. For both species, we set the values of parameters controlling the water  
1059 retention (i.e.  $B_{cap}$  and  $D_s$ , Appendix B) and the water-stress effects on net photosynthesis (i.e.  
1060  $W_{cap}$ , Eq. 4) to be the same as those in *S. magellanicum* (Test 3) or same as those in *S. fallax* (Test  
1061 4). Our hypothesis would be supported if removing the interspecific differences in  $RWC$  responses  
1062 led to the failure to predict the habitat preferences of the species.

1063 We implemented Tests 5-6 to test the importance of parameters that directly control the species  
1064 ability to overgrow another species with the more rapid height increment (i.e.  $Pm_{20}$ ,  $RS_{20}$ ,  $\alpha_{PPFD}$   
1065 and  $H_{spec}$ ) in lawn and hummock conditions to the habitat preferences of the species. We eliminated  
1066 the species differences in the parameter values to be same as those in *S. magellanicum* (Test 5)  
1067 and same as those in *S. fallax* (Test 6). The effects of the manipulation on the simulated habitat  
1068 preferences were compared against those from Tests 3-4. For each of Tests 3-6, 80 Monte-Carlo  
1069 simulations were run using the setups described in Test 1.

1070

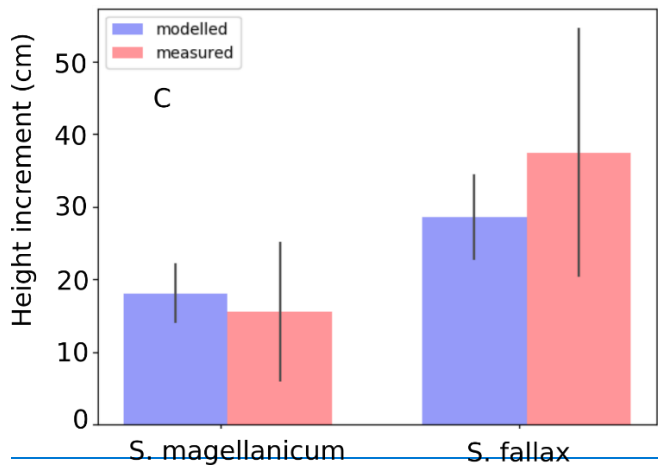
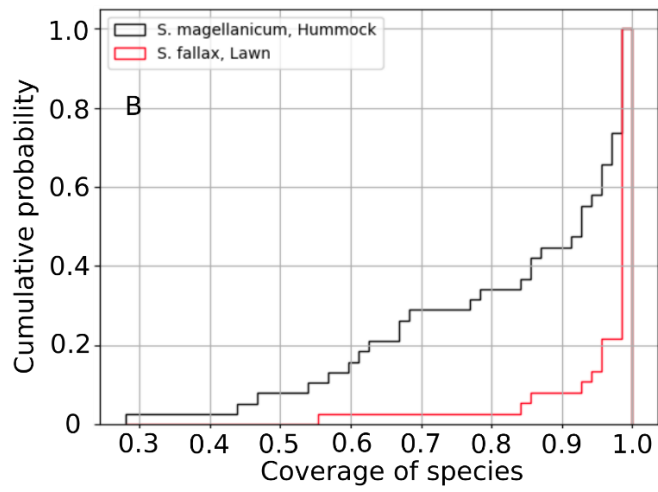
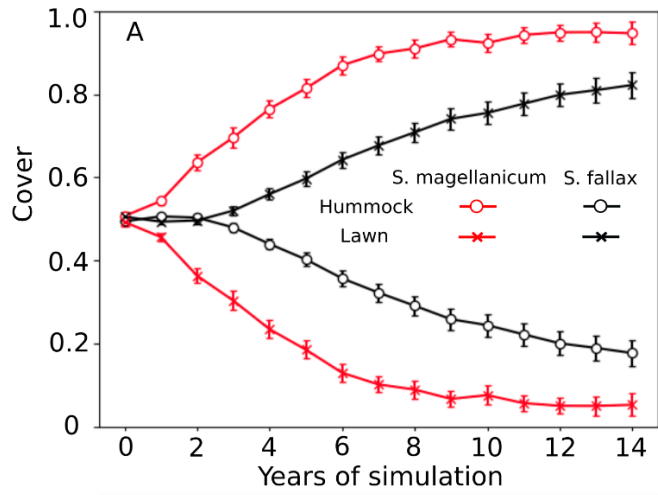
## 1071 **3 Results**

### 1072 **3.1 Simulating the habitat preferences of *Sphagnum* species as affected by water retention**



1073 **traits of capitulum**

1074 Test 1 showed the ability of model to capture the preference of *S. magellanicum* for the hummock  
1075 environment and *S. fallax* for the lawn environment (Fig. 2A). The simulated annual changes in  
1076 species covers were greater in lawn than in hummock habitats during the first 5 simulation years.  
1077 The changes in lawn habitats slowed down around year 10 and the cover of *S. fallax* plateaued at  
1078 around  $95\pm 2.8\%$  (mean  $\pm$  standard error). In contrast, the cover of *S. magellanicum* on hummocks  
1079 continued to grow until the end of simulation and reached  $83\pm 3.1\%$ . In the lawn habitats, the cover  
1080 of *S. fallax* increased in all Monte-Carlo simulations and the species occupied all grid cells in 70%  
1081 of the simulations. In the hummock habitats, the cover of *S. magellanicum* increased in 91% of  
1082 Monte-Carlo simulations, and formed monocultural community in 16% of simulations (Fig. 2B).  
1083 The height growth of *Sphagnum* mosses was significantly greater at lawns than at hummocks  
1084 ( $P < 0.01$ ). The ranges of simulated height growths agreed well with the observed values from field  
1085 measurement for both species (Fig. 2C).

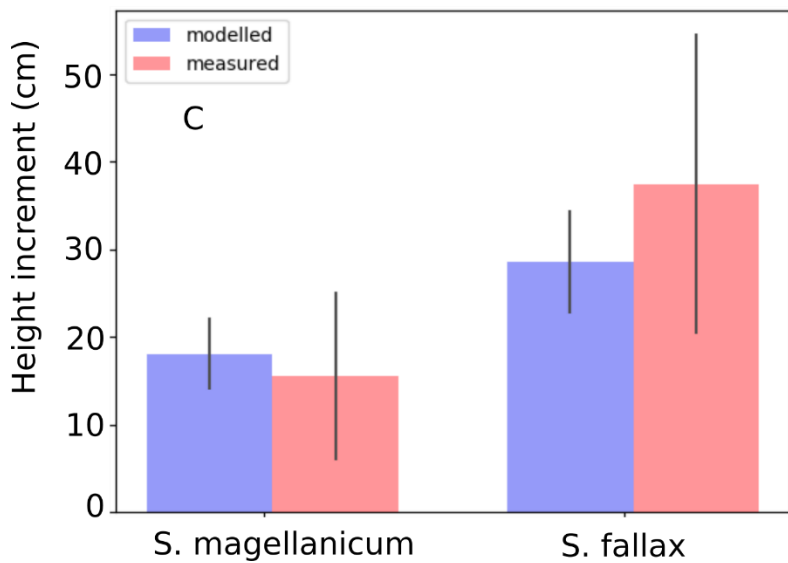
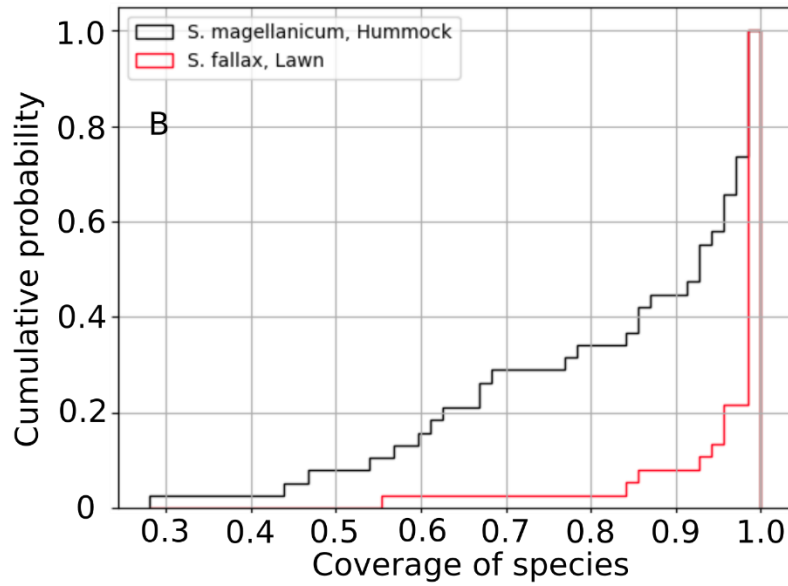
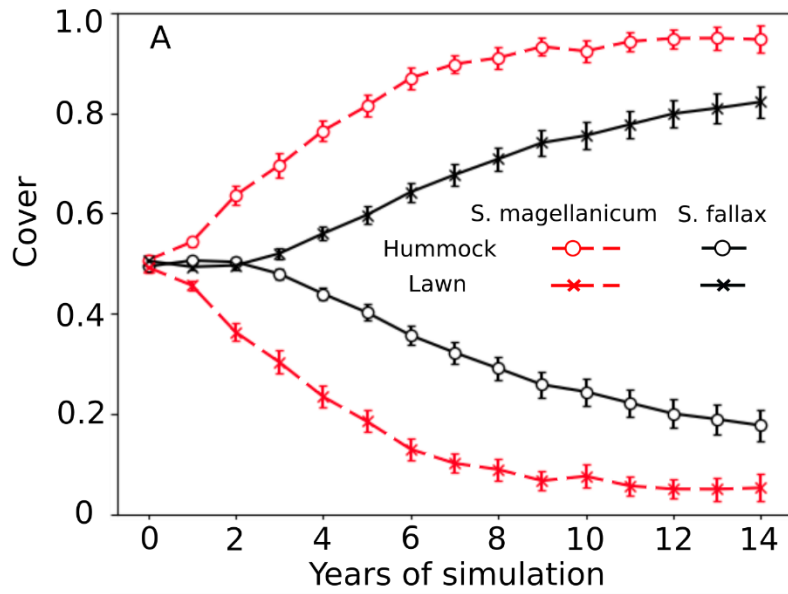


1086

1087

1088





1090 Figure 2. Testing the ability of PCS to predict habitat preference of *Sphagnum magellanicum* and  
1091 *S. fallax* (Test 1). The hummock and lawn habitats were differentiated by water table depth, surface  
1092 energy balances and capitulum water potential in modelling. In the beginning of simulation, the  
1093 cover of the two species was set equal and it was allowed to develop with time. (A) Annual  
1094 development of the [relative](#) cover (mean and standard error) of the two species in hummock and  
1095 lawn habitats, (B) the cumulative probability distribution of the cover of the two species at the end  
1096 of the 15-year period based on 80 Monte-Carlo simulations, and (C) the simulated and measured  
1097 means of annual height growth of *Sphagnum* surfaces in [their natural habitats in](#) hummock and  
1098 lawn habitats.

1099

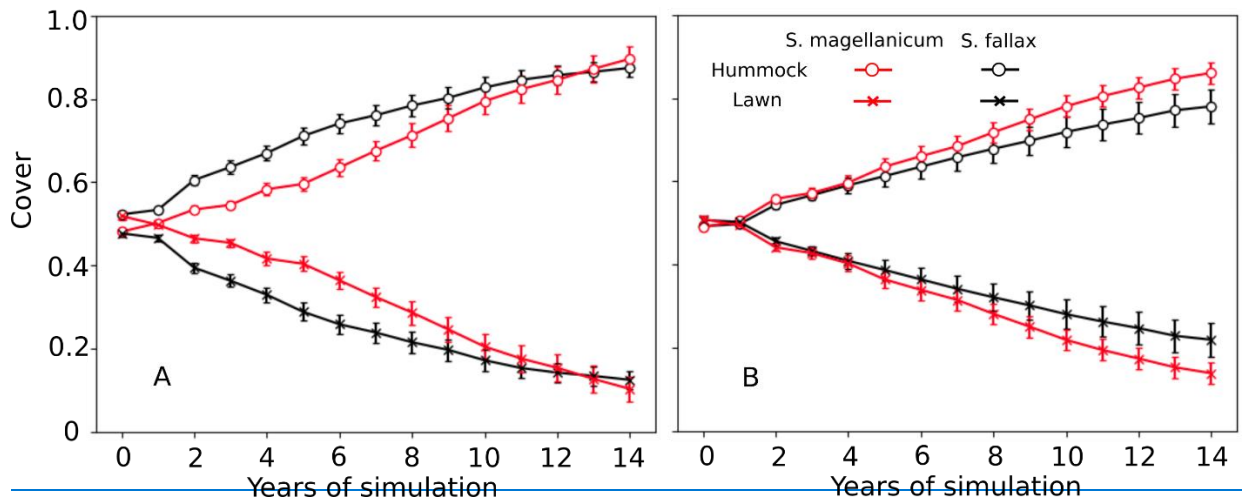
### 1100 **3.2 Testing model robustness**

1101 Test 2 addressed the model robustness to the uncertainties in several parameters that closely linked  
1102 to hydrology and growth calculations. Modifying most of the parameter values by +10% or -10%  
1103 yielded marginal changes in the mean cover of species in either hummock or hollow habitat (Table:  
1104 [34](#)). Reducing the moss carpet and peat hydraulic parameter *n* had stronger impacts on *S. fallax*  
1105 cover in hummocks than in lawns. Nevertheless, changes in simulated cover that were caused by  
1106 parameter manipulations were generally smaller than the standard deviations of the means [i.e.](#)  
1107 [fitting into the random variation](#).

1108

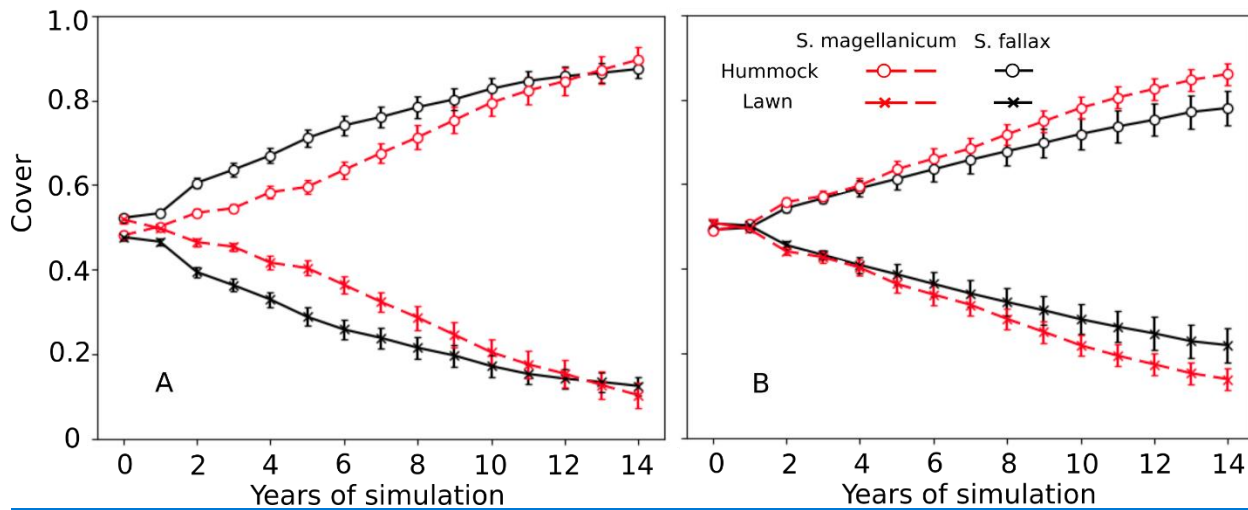
### 1109 **3.3 Testing the controlling role of capitulum water retention for community dynamics**

1110 In Tests 3 and 4, the model incorrectly predicted the competitiveness of two species when the  
1111 interspecific differences of capitulum water retention were eliminated. In both tests, *S. fallax*  
1112 became dominant in all habitats. The use of water responses characteristic to *S. magellanicum* for  
1113 both species (Test 3) led to faster development of *S. fallax* cover and higher coverage at the end of  
1114 simulation (Fig. 3A), as compared with the simulation results where the water responses  
1115 characteristic to *S. fallax* were used for both species (Test 4, Fig. 3B). The pattern was more  
1116 pronounced in hummock than in lawn habitats.



1117

1118



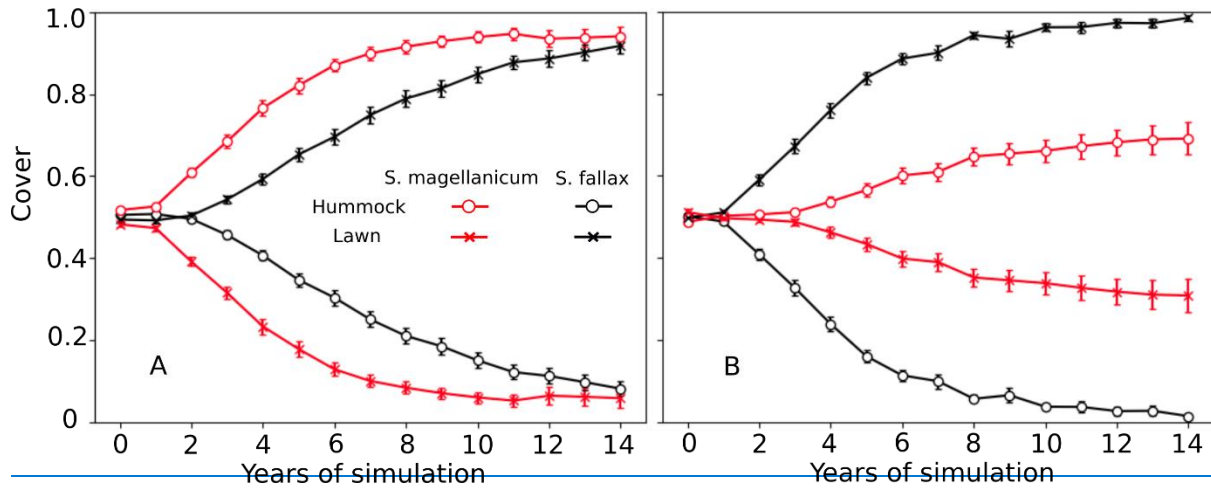
1119

1120 Figure 3. Testing the importance of capitulum water retention to the habitat preference of *S.*  
 1121 *magellanicum* and *S. fallax*. The development of [the relative cover](#) (mean and standard error) were  
 1122 simulated in hummock and lawn habitats over a 15-year time frame for the two species. For both  
 1123 species, parameter values for the capitulum water retention, capitulum biomass ( $B_{cap}$ ) and density  
 1124 ( $D_S$ ) were set to be the same as those from (A) *S. magellanicum* (Test 3) or (B) *S. fallax* (Test 4).

1125

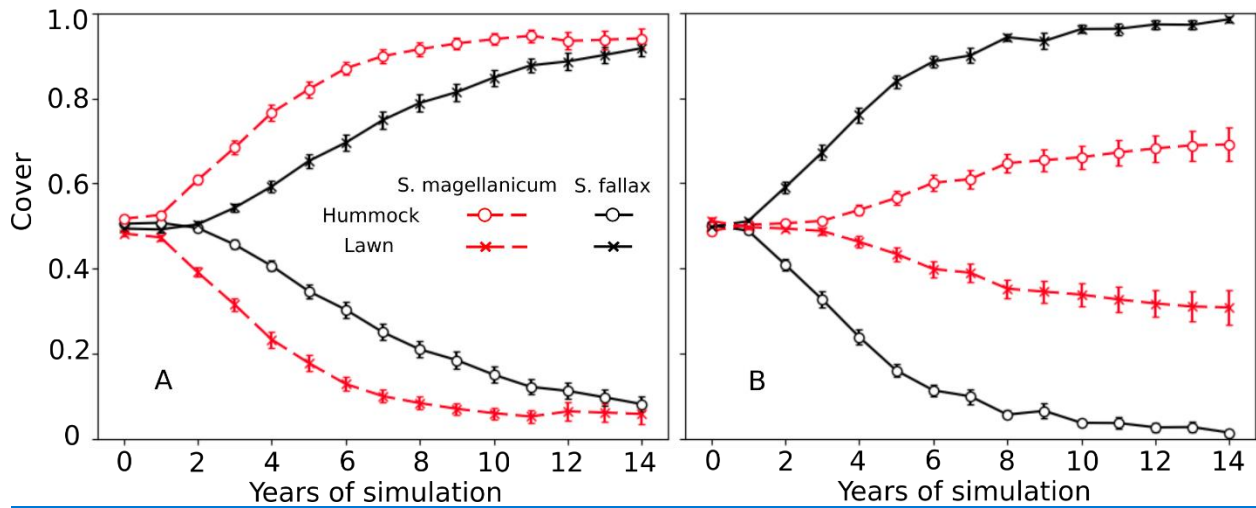
1126 In Tests 5 and 6, the species differences in the growth-related parameters were eliminated.  
 1127 However, the model still predicted the dominances of *S. fallax* and *S. magellanicum* in lawn and  
 1128 hummock habitats, respectively (Fig. 4). The increase in the mean cover of *S. magellanicum* was  
 1129 especially fast in hummock habitat in comparison to the results of the unchanged model from Test  
 1130 1 (Fig. 2A). In lawns, the use of *S. fallax* growth parameters for both species gave stronger  
 1131 competitiveness to *S. magellanicum* (Fig. 4B) than using the *S. magellanicum* parameters (Fig.  
 1132 4A).

1133



1134

1135



1136

1137 Figure 4. Testing the importance of parameters regulating net photosynthesis and shoot elongation  
 1138 to the habitat preference of *S. magellanicum* and *S. fallax*. Annual development of the [relative](#)  
 1139 cover (mean and standard error) of the two species were simulated for hummock and lawn habitats  
 1140 over a 15-year time frame. For both species, the parameter values (i.e.  $Pm_{20}$ ,  $RS_{20}$ ,  $\alpha_{PPFD}$  and  $H_{spec}$ )  
 1141 were set to be the same as those from (A) *S. magellanicum* (Test 5) or (B) *S. fallax* (Test 6).

1142

1143 **4 Discussion**

1144 In peatland ecosystems, *Sphagnum* are keystone species differentially distributed primarily along  
 1145 the hydrological gradient ([e.g. Andrus et al. 1986; Rydin, 1986](#)). In a context where substantial  
 1146 change in peatland hydrology is expected under a changing climate in northern area (e.g. longer  
 1147 snow-free season, lower summer water table and more frequent droughts), there is a pressing need  
 1148 to understand how peatland plant communities could react and how *Sphagnum* species could

1149 redistribute under habitat changes. In this work, we developed Peatland Moss Simulator (PMS), a  
1150 process-based stochastic model, to simulate the competition between *S. magellanicum* and *S.*  
1151 *fallax*, two key species representing dry (hummock) and wet (lawn) habitats in a poor fen peatland.  
1152 We empirically showed that these two species differed in characteristics that likely affect their  
1153 competitiveness. The capitulum water retention for the lawn-preferring species (*S. fallax*) was  
1154 weaker than that for the hummock-preferring species (*S. magellanicum*). Compared to *S.*  
1155 *magellanicum*, the capitula of *S. fallax* held less water at saturation and water content decreased  
1156 more rapidly with dropping water potential. Hence, *S. fallax* would dry faster than *S. magellanicum*  
1157 under the same rate of water loss. Moreover, the water content in *S. fallax* capitula was less  
1158 resistant to evaporation. These differences indicated that it is harder for *S. fallax* capitula to buffer  
1159 evaporative loss of water and thereby avoid or delay desiccation. [Similar differences between](#)  
1160 [hummock and hollow species have been found also earlier \(Titus & Wagner, 1984; Rydin &](#)  
1161 [McDonald, 1985\).](#) In addition, the net photosynthesis of *S. fallax* is more sensitive to changes in  
1162 capitulum water content than *S. magellanicum* [as seen in steeper decline in photosynthesis with](#)  
1163 [decreasing water content \(Fig. B2C\).](#) Consequently, *S. fallax* is more likely to be constrained by  
1164 dry periods, when the capillary water cannot fully compensate the evaporative loss (Robroek et  
1165 al., 2007b) making it less competitive in habitats prone to desiccation. The PMS successfully  
1166 captured the habitat preferences of the two *Sphagnum* species (Test 1): starting from a mixed  
1167 community with equal probabilities for both species, the lawn habitats with shallower water table  
1168 were eventually dominated by the typical lawn species *S. fallax*, whereas hummock habitats, which  
1169 were 15 cm higher than the lawn surface, were taken over by *S. magellanicum*. The low final cover  
1170 of *S. magellanicum* simulated in lawn habitats agreed well with [our field](#) observation from [the our](#)  
1171 study site, where *S. magellanicum* cover was less than 1% [over in lawns mesocosms](#) (Kokkonen  
1172 et al., 2019). On the other hand, *S. fallax* was outcompeted by *S. magellanicum* in the hummock  
1173 habitats. This result is consistent with previous findings that hollow-preferring *Sphagna* are less  
1174 likely to survive in hummock environments with greater drought pressure (see Rydin 1985; Rydin  
1175 et al. 2006; Johnson et al., 2015). The simulated annual height increments of mosses also agreed  
1176 well with the observed values for both habitat types. [As was the case in our simulation for lawn](#)  
1177 [habitat, the looser stem structure of S. fallax, allows it to allocate more of the produced biomass](#)  
1178 [into height growth and therein overgrow S. magellanicum that allocates the produced biomass to](#)  
1179 [form compact stem, packed with thick fascicles.](#) This indicated that PMS can capture key  
1180 mechanisms in controlling the growth and interactions of the *Sphagnum* species.

1181 The testing of parameter sensitivity showed the robustness of PMS regarding the uncertainties  
1182 in parameterization, as the simulated changes in the mean species cover were generally less than  
1183 the standard deviations of the means under 10% changes in several parameters. We found that  
1184 decreasing the value of hydraulic parameter  $n$  increased the presence of *S. fallax* in the hummock  
1185 habitats. This was expected [as  \$n\$  is a scaling factor and therefore its changes get magnified](#): a lower  
1186  $n$  value will lead to higher water content in the unsaturated layers (van Genuchten, 1978), which

1187 is important to wet-adapted *Sphagna* in order to survive dry conditions (Hayward and Clymo,  
1188 1982; Robroek et al., 2007b; Rice et al., 2008). In contrast, the response of *Sphagnum* cover to the  
1189 changes in other hydraulic parameters (i.e.  $\alpha$ ,  $n$ ,  $K_h$ ) were limited in lawn habitats. This could be  
1190 due to the relatively shallow water table in lawns, which was able to maintain sufficient capillary  
1191 rise to the moss carpet and capitula. Decreasing the values of  $k_{imm}$  and  $NSC_{max}$  mainly decreased  
1192 the cover of *S. fallax* in lawn habitats, consistent with the importance of biomass production to  
1193 *Sphagna* in high moisture environment (e.g. Rice et al., 2008; Laine et al., 2011). In addition, the  
1194 SVAT modelling for hummocks and lawns (Module III, Fig. 1) employed same hydraulic  
1195 parameter values obtained from *S. magellanicum* hummocks (McCarter and Price, 2014). This  
1196 could overestimate  $K_m$  but underestimate  $n$  for lawns, as the lawn peat could be less efficient in  
1197 water retention and capillary-flow generation, as compared to hummock peat (Robroek et al.,  
1198 2007b; Branham and Strack, 2014). As the decrease in  $K_m$  and increase in  $n$  showed counteracting  
1199 effects on the simulated species covers (Table: 34), the biases in the parameterization of  $K_m$  and  $n$   
1200 may not critically impact model performance.

1201 Both our empirical measurements and PMS simulations indicate the importance of capitulum  
1202 water retention as a mechanism controlling the moss community dynamics in peatlands. It has long  
1203 been hypothesized and experimentally studied that *Sphagnum* niche is defined by two processes.  
1204 Firstly, Dry, high elevation habitats such as hummocks; physically select species with ability to  
1205 remain moist (Rydin, 1993). ~~On the one hand, o~~ If the interspecific differences in water retention  
1206 and water-stress effects were correctly specified (Test 1) o Our model predicted this phenomena  
1207 of the stronger competitiveness of *S. magellanicum* against *S. fallax* in their preferred hummock  
1208 habitats correctly ~~the competitiveness of *S. magellanicum* against *S. fallax* in their preferred~~  
1209 ~~habitats, if the interspecific differences in water retention and water-stress effects were correctly~~  
1210 ~~specified (Test 1).~~ Alternatively, the model failed to predict the distribution of *S. magellanicum* on  
1211 hummocks, if these interspecific differences were neglected (Test 3 and Test 4, Fig. 3). ~~This could~~  
1212 ~~be because the capillary rise during~~ During low water-table periods in summer the capillary rise  
1213 may not fully compensate for the high evaporation (Robroek et al., 2007b; Nijp et al., 2014). In  
1214 such circumstances, capitulum water potential could drop rapidly towards the pressure defined by  
1215 the relative humidity of air (Hayward and Clymo, 1982). ~~It has long been hypothesized and~~  
1216 ~~experimentally studied that *Sphagnum* niche is defined by two processes. Dry, high elevation~~  
1217 ~~habitats such as hummocks, physically select species with ability to remain moist (Rydin, 1993).~~  
1218 Consequently, the ability of capitula to retain cytoplasmic water would be particularly important  
1219 for the hummock-preferring species, as was also shown by Titus & Wagner (1984). Secondly, On  
1220 the other hand, in habitats with high moisture content such as lawns and hollows, the interspecific  
1221 competition becomes important: ~~and~~ it is well acknowledged that species from such habitats  
1222 generally have a higher growth rate and photosynthetic capacity compared to hummock species is  
1223 important to the competitiveness of *Sphagna* in habitats of high moisture content (e.g. Laing et al.,  
1224 2014; Bengtsson et al., 2016). Our results also agreed on this, as setting the growth-related



1225 parameters (i.e.  $Pm_{20}$ ,  $RS_{20}$ ,  $\alpha_{PPFD}$  and  $H_{spec}$ ) of *S. magellanicum* to be the same as those of *S. fallax*  
1226 decreased the *S. fallax* cover in both hummock and lawn habitats (Test 6, Fig. 4B). However, the  
1227 model still captured the habitat preferences for the tested species without including the  
1228 interspecific differences in those growth-related parameters. Based on this, the growth-related  
1229 parameters could be less important than those water-related ones.

1230 There have been growing concerns on the shift of peatland communities from *Sphagnum*-  
1231 dominated towards more vascular-abundant under a drier and warmer climate (Wullschleger et  
1232 al., 2014; Munir et al. 2015; Dieleman et al. 2015). Nevertheless, the potential of *Sphagnum*  
1233 species composition to adjust to this forcing remains poorly understood. Particularly in  
1234 oligotrophic fens where the vegetation is substantially shaped by lateral hydrology (Tahvanainen,  
1235 2011; Turetsky et al., 2012), plant communities can be highly vulnerable to hydrological changes  
1236 (Gunnarsson et al. 2002; Tahvanainen, 2011). Based on the validity and robustness of PMS, we  
1237 believe PMS could serve as one of the first mechanistic tools to investigate the direction and rate  
1238 of *Sphagnum* communities to change under environmental forcing. The hummock-lawn  
1239 differences showed by Test 1 implied that *S. magellanicum* could outcompete *S. fallax* within a  
1240 decadal time frame in a poor fen community, if the water table of habitats like lawns was lowered  
1241 by 15 cm (Test 1). Although this was derived from a simplified system with only the two species,  
1242 it highlighted the potential of rapid turnover of *Sphagnum* species: the hummock-lawn difference  
1243 of water table in simulation was comparable to the expected water table drawdown in fens under  
1244 the warming climate (Whittington and Price, 2006; Gong et al., 2013b). [The effect traits of mosses,  
1245 while studied less than those of vascular plant traits, have far reaching impacts on biogeochemistry  
1246 of ecosystems such as peatlands, where mosses form the most significant plant group \(Cornelissen  
1247 et al. 2007\).](#) Because of the large interspecific differences of traits such as photosynthetic potential,  
1248 hydraulic properties and litter chemistry (Laiho 2006; Straková et al., 2011; Korrensalo et al.,  
1249 2017; Jassej & Signarbieux, 2019), change in *Sphagnum* community composition is likely to  
1250 impact long-term peatland stability and functioning (Waddington et al., 2015). [Turnover between  
1251 hummock and wetter habitat species would feedback to climate as they differ in their  
1252 decomposability \(Straková et al. 2012; Bengtsson et al. 2016\). As hummock species produces  
1253 more calcitrant litter the carbon bind into the system would take longer to get released back to  
1254 atmosphere. In addition, the replacement of wet adapted moss species with hummock species is  
1255 likely to result in higher ability to maintain carbon sink under periods of drought \(Jassej, &  
1256 Signarbieux, 2019\).](#)

1257 Although efforts have been made on analytical modelling to obtain boundary conditions for  
1258 equilibrium states of moss and vascular communities in peatland ecosystems (Pastor et al., 2002),  
1259 the dynamical process of peatland vegetation has not been well-described or included in earth  
1260 system models (ESMs). Existing ecosystem models usually consider the features of peatland moss  
1261 cover as “fixed” (Sato et al., 2007; Wania et al., 2009; Euskirchen et al., 2014), or change  
1262 directionally following a projected trajectory (Wu and Roulet, 2014). Our modelling approach

1263 provided a way to incorporate the mechanisms of dynamical moss cover into peatland carbon  
1264 modelling, ~~and thus may serve the wider research community working on global biogeochemical~~  
1265 ~~eyeles.~~ **PCSPMS** employed an individual-based approach where each grid cell carries a unique set  
1266 of trait properties, so that shoots with favorable trait combinations in prevailing environment are  
1267 thus able to replace those whose trait combinations are less favorable. This mimic the stochasticity  
1268 in plant responses to environmental fluctuations, which are essential to community assembly and  
1269 trait filtering under environmental forcing (Clark et al., 2010). Moreover, the model included the  
1270 spatial interactions of individuals, which can impact the sensitivity of coexistence pattern to  
1271 environmental changes (Bolker et al., 2003; Sato et al., 2007; Tatsumi et al., 2019). Because these  
1272 features are essential to the “next generation” DVMs (Scheiter et al., 2013), PMS **with competition**  
1273 **based on growth rates** could be considered as an elemental design for future DVM development.

1274 To conclude, our PMS could successfully capture the habitat preferences of the modelled  
1275 *Sphagnum*. In this respect, our PMS model could provide fundamental support for the future  
1276 development of dynamic vegetation models for peatland ecosystems. Based on our findings, the  
1277 capitulum water processes should be considered as a control on the vegetation dynamics in future  
1278 impact studies on peatlands under changing environmental conditions.

1279

## 1280 **Acknowledgements**

1281 We are grateful to Harri Strandman (University of Eastern Finland) for the coding of Weather  
1282 Generator. The project was funded by Academy of Finland (287039). **AML** acknowledges support  
1283 from the Kone Foundation and SF from grant #1802825 from the US National Science Foundation,  
1284 and the Fulbright-Finland and Saastamoinen Foundations.

1285

1286 *Code and data availability.* The data and the code to reproduce the analysis is available upon  
1287 request to the corresponding author.

1288 *Author contributions.* JG and EST designed the study. JG, AML and NK conducted the experiment  
1289 and analysis. JG, EST, NR and SF designed the model. JG coded the model and conducted the  
1290 model simulation and data analysis. JG wrote the manuscript with contributions from all co-  
1291 authors.

1292 *Competing interests.* The authors declare that they have no conflict of interest.

1293

## 1294 **References**

1295 Alm, J., Shurpali, N. J., Tuittila, E.-S., Laurila, T., Maljanen, M., Saarnio, S. and Minkkinen, K.:  
1296 Methods for determining emission factors for the use of peat and peatlands – flux measurements  
1297 and modelling, *Boreal Environment Research*, 12, 85-100, 2007.



- 1298 Amarasekare, P.: Competitive coexistence in spatially structured environments: A synthesis,  
1299 Ecology Letters, 6, 1109-1122, 2003.
- 1300 Anderson K. and Neuhauser C.: Patterns in spatial simulations—are they real? Ecological  
1301 Modelling, 155, 19-30, 2000.
- 1302 Andrus R. E.: Some aspects of Sphagnum ecology, Can. J. Bot., 64, 416–426, 1986.
- 1303 Asaeda, T. and Karunaratne, S.: Dynamic modelling of the growth of Phragmites australis: model  
1304 description, Aquatic Botany, 67, 301-318, 2000.
- 1305 Bengtsson, F., Granath, G. and Rydin, H.: Photosynthesis, growth, and decay traits in Sphagnum  
1306 - a multispecies comparison. Ecology and Evolution, 6, 3325-3341, 2016.
- 1307 Blois, J. L., Williams, J. W., Fitzpatrick, M. C., Jackson, S. T. and Ferrier S.: Space can substitute  
1308 for time in predicting climate-change effects on biodiversity, PNAS, 110, 9374-9379,  
1309 doi:10.1073/pnas.1220228110, 2013.
- 1310 Breeuwer, A., Heijmans, M. M., Robroek, B. J., Berendse, F. (2008). The effect of temperature on  
1311 growth and competition between Sphagnum species. Oecologia, 156(1), 155-67.
- 1312 Bolker, B. M., Pacala, S. W. and Neuhauser, C.: Spatial dynamics in model plant communities:  
1313 What do we really know? Am. Nat., 162, 135–148, 2003.
- 1314 Boulangeat, I., Svenning, J. C., Daufresne, T., Leblond, M. and Gravel, D.: The transient response  
1315 of ecosystems to climate change is amplified by trophic interactions, Oikos, 127, 1822–1833,  
1316 2018.
- 1317 Branham, J. E. and Strack, M.: Saturated hydraulic conductivity in *Sphagnum*-dominated  
1318 peatlands: do microforms matter? Hydrol. Process., 28, 4352-4362, 2014.
- 1319 Chesson, P. (2000). General theory of competitive coexistence in spatially varying environments.  
1320 Theoretical Population Biology 58, 211–237.
- 1321 Clapp, R. B., Hornberger, G. M. (1978). Empirical equations for some soil hydraulic properties.  
1322 Water Resour. Res, 14, 601–604.
- 1323 Clark J. S., Bell D., Chu C., Courbaud B., Dietze M., Hersh M., HilleRisLambers J., Ibanez I.,  
1324 LaDeau S., McMahon S., Metcalf, J., Mohan, J., Moran, E., Pangle, L., Pearson, S., Salk, C., Shen,  
1325 Z., Valle, D. and Wyckoff, P.: High-dimensional coexistence based on individual variation: a  
1326 synthesis of evidence, Ecological Monographs, 80, 569 – 608, 2010.
- 1327 Clymo, R. S.: The growth of Sphagnum: Methods of measurement, Journal of Ecology, 58, 13-49,  
1328 1970.

- 1329 [Cornelissen, J. H., Lang, S. I., Soudzilovskaia, N. A., and During, H. J.: Comparative cryptogam](#)  
1330 [ecology: a review of bryophyte and lichen traits that drive biogeochemistry. \*Annals of botany\*,](#)  
1331 [99\(5\), 987-1001, 2007](#)  
1332
- 1333 Czárán T. and Iwasa Y.: Spatiotemporal models of population and community dynamics, *Trends*  
1334 *Ecol. Evol.*, 13, 294–295, 1998.
- 1335 Dieleman, C. M., Branfireun, B. A., Mclaughlin, J. W. and Lindo, Z.: Climate change drives a  
1336 shift in peatland ecosystem plant community: Implications for ecosystem function and stability,  
1337 *Global Change Biology*, 21, 388-395, 2015.
- 1338 Euskirchen, E. S., Edgar, C. W., Turetsky, M. R., Waldrop, M. P. and Harden J. W.: Differential  
1339 response of carbon fluxes to climate in three peatland ecosystems that vary in the presence and  
1340 stability of permafrost, *J. Geophys. Res. Biogeosci.*, 119, 1576–1595, 2014.
- 1341 Frohking, S., Roulet, N. T., Moore, T. R., Lafleur, T. M., Bubier, L. J. and Crill, P. M.: Modeling  
1342 seasonal to annual carbon balance of Mer Bleue Bog, Ontario, Canada. *Global Biogeochem.*  
1343 *Cycles*, 16, doi:10.1029/2001GB001457, 2002.
- 1344 Gassmann, F., Klötzli, F. and Walther, G.: Simulation of observed types of dynamics of plants and  
1345 plant communities, *Journal of Vegetation Science*, 11, 397 – 408, 2003.
- 1346 Goetz, J. D., Price, J. S. (2015). Role of morphological structure and layering of *Sphagnum* and  
1347 *Tomenthypnum* mosses on moss productivity and evaporation rates. *Canadian Journal of Soil*  
1348 *Science*, 95, 109-124.
- 1349 ~~Gong, J., Kokkonen, N., Laine, A. M. and Tuittila, E. S.: *Sphagnum capitula* water retention as a~~  
1350 ~~controlling mechanism for peatland moss community dynamics, *Biogeosciences Discussion*, bg-~~  
1351 ~~2019-331, 2019 (submitted manuscript).~~
- 1352 Gong, J., Shurpali, N., Kellomäki, S., Wang, K., Salam, M. M. and Martikainen, P. J.: High  
1353 sensitivity of peat moisture content to seasonal climate in a cutaway peatlandcultivated with a  
1354 perennial crop (*Phalaris arundinacea*, L.): a modeling study, *Agricultural and Forest Meteorology*,  
1355 180, 225–235, 2013a.
- 1356 Gong, J., Wang, K., Kellomäki, S., Wang, K., Zhang, C., Martikainen, P. J. and Shurpali, N.:  
1357 Modeling water table changes in boreal peatlands of Finland under changing climate conditions,  
1358 *Ecological Modelling*, 244, 65-78, 2013b.
- 1359 Gong, J., Jia, X., Zha, T., Wang, B., Kellomäki, S. and Peltola, H.: Modeling the effects of plant-  
1360 interspace heterogeneity on water-energy balances in a semiarid ecosystem, *Agricultural and*  
1361 *Forest Meteorology*, 221, 189–206, 2016.
- 1362 Gorham, E.: Northern peatlands: Role in the carbon cycle and probable responses to climatic  
1363 warming, *Ecol. Appl.*, 1, 182–195, 1991.

- 1364 Gunnarsson, U., Malmer, N. and Rydin, H.: Dynamics or constancy in Sphagnum dominated mire  
1365 ecosystems? A 40-year study, *Ecography*, 25, 685–704, 2002.
- 1366 Hartmann, H. and Trumbore, S.: Understanding the roles of nonstructural carbohydrates in forest  
1367 trees – from what we can measure to what we want to know, *New Phytol*, 211, 386-403, 2016.
- 1368 Hájek, T. and Beckett, R. P.: Effect of water content components on desiccation and recovery in  
1369 Sphagnum mosses, *Annals of Botany*, 101, 165–173, 2008.
- 1370 Hájek, T., Tuittila, E.-S., Ilomets, M. and Laiho, R.: Light responses of mire mosses - A key to  
1371 survival after water-level drawdown? *Oikos*, 118, 240-250, 2009.
- 1372 Hayward P. M. and Clymo R. S.: Profiles of water content and pore size in Sphagnum and peat,  
1373 and their relation to peat bog ecology. *Proceedings of the Royal Society of London, Series B,*  
1374 *Biological Sciences*, 215, 299-325, 1982.
- 1375 Hayward P. M. and Clymo R. S.: The growth of Sphagnum: experiments on, and simulation of,  
1376 some effects of light flux and water-table depth. *Journal of Ecology*, 71, 845-863, 1983.
- 1377 Holmgren, M., Lin, C., Murillo, J. E., Nieuwenhuis, A., Penninkhof, J., Sanders, N., Bart, T., Veen,  
1378 H., Vasander, H., Vollebregt, M. E. and Limpens, J.: Positive shrub–tree interactions facilitate  
1379 woody encroachment in boreal peatlands, *J. Ecol.*, 103, 58-66, 2015.
- 1380 Hugelius, G., Tarnocai, C., Broll, G., Canadell, J. G., Kuhry, P. and Swanson, D. K.: The Northern  
1381 Circumpolar Soil Carbon Database: spatially distributed datasets of soil coverage and soil carbon  
1382 storage in the northern permafrost regions, *Earth Syst. Sci. Data*, 5, 3-13, 2013.
- 1383 Jassey, V. E., & Signarbieux, C.: Effects of climate warming on Sphagnum photosynthesis in  
1384 peatlands depend on peat moisture and species-specific anatomical traits. *Global change biology*,  
1385 25(11), 3859-3870, 2019.
- 1386 Johnson, M. G., Granath, G., Tahvanainen, T., Pouliot, R., Stenøien, H. K., Rochefort, L., Rydin,  
1387 H. and Shaw, A. J.: Evolution of niche preference in Sphagnum peat mosses, *Evolution*, 69, 90 –  
1388 103, 2015.
- 1389 Kellomäki, S. and Väisänen, H.: Modelling the dynamics of the forest ecosystem for climate  
1390 change studies in the boreal conditions, *Ecol. Model.*, 97, 121-140, 1997.
- 1391 Keuper, F., Dorrepaal, E., Van Bodegom, P. M., Aerts, R., Van Logtestijn, R. S.P., Callaghan, T.  
1392 V. and Cornelissen, J. H.C.: A Race for Space? How Sphagnum fuscum stabilizes vegetation  
1393 composition during long-term climate manipulations, *Global Change Biology*, 17, 2162–2171,  
1394 2011.
- 1395 Kokkonen, N., Laine, A., Laine, J., Vasander, H., Kurki, K., Gong, J. and Tuittila, E.-S.: Responses  
1396 of peatland vegetation to 15-year water level drawdown as mediated by fertility level. *J. Veg. Sci.*,  
1397 [30\(6\), 1206-1216](#)[DOI: 10.1111/jvs.12794](#), 2019. ~~(accepted manuscript)~~.

- 1398 [Korrensalo, A., Hájek, T., Vesala, T., Mehtätalo, L., & Tuittila, E. S. \(2016\). Variation in](#)  
1399 [photosynthetic properties among bog plants. \*Botany\*, 94\(12\), 1127-1139.](#)
- 1400 Korrensalo, A., Alekseychik, P., Hájek, T., Rinne, J., Vesala, T., Mehtätalo, L., Mammarella, I.  
1401 and Tuittila, E.-S.: Species-specific temporal variation in photosynthesis as a moderator of  
1402 peatland carbon sequestration, *Biogeosciences*, 14, 257-269, 2017.
- 1403 Kyrkjeeide, M. O., Hassel, K., Flatberg, K. I., Shaw, A. J., Yousefi, N. and Stenøien, H. K. Spatial  
1404 genetic structure of the abundant and widespread peatmoss *Sphagnum magellanicum* Brid. *PLoS*  
1405 *One*, 11, e0148447, 2016.
- 1406 Laiho, R. Decomposition in peatlands: Reconciling seemingly contrasting results on the impacts  
1407 of lowered water levels, *Soil Biology and Biochemistry*, 38, 2011-2024, 2006.
- 1408 Laine, A. M. Juurola, E., Hájek, T., Tuittila, E.-S. (2011). *Sphagnum* growth and ecophysiology  
1409 during mire succession. *Oecologia*, 167: 1115-1125.
- 1410 Laine, J., Komulainen, V.-M., Laiho, R., Minkkinen, K., Ras-  
1411 Sarkkola, S., Silvan, N., Tolonen, K., Tuittila, E.-S., Vasander, H., and Päivänen, J. (2004).  
1412 *Lakkasuo – a guide to mire ecosystem*, Department of Forest Ecology Publications, University of  
1413 Helsinki, 31, 123 pp.
- 1414 Laine, J., Flatberg, K. I., Harju, P., Timonen, T., Minkkinen, K., Laine, A., Tuittila, E.-S.,  
1415 Vasander, H. (2018) *Sphagnum Mosses — The Stars of European Mires*. University of Helsinki  
1416 Department of Forest Sciences, *Sphagna Ky*. 326 p.
- 1417 Laine J., Harju P., Timonen T., Laine A., Tuittila E.-S., Minkkinen K. and Vasander H.: The  
1418 intricate beauty of *Sphagnum* mosses—a Finnish guide to identification (Univ Helsinki Dept Forest  
1419 Ecol Publ 39). Department of Forest Ecology, University of Helsinki, Helsinki, pp 1–190, 2009.
- 1420 Laing, C. G., Granath, G., Belyea, L. R., Allton K. E. and Rydin, H.: Tradeoffs and scaling of  
1421 functional traits in *Sphagnum* as drivers of carbon cycling in peatlands, *Oikos*, 123, 817–828,  
1422 2014.
- 1423 Larcher, W.: *Physiological Plant Ecology: Ecophysiology and Stress Physiology of Functional*  
1424 *Groups*, Springer, 2003.
- 1425 Letts, M. G., Roulet, N. T. and Comer, N. T.: Parametrization of peatland hydraulic properties for  
1426 the Canadian land surface scheme, *Atmosphere-Ocean*, 38, 141-160, 2000.
- 1427 Martínez-Vilalta, J., Sala, A., Asensio, D., Galiano, L., Hoch, G., Palacio, S., Piper, F. I. and Lloret,  
1428 F.: Dynamics of non-structural carbohydrates in terrestrial plants: a global synthesis. *Ecol Monogr*,  
1429 86, 495-516, 2016.
- 1430 McCarter C. P. R. and Price J. S.: Ecohydrology of *Sphagnum* moss hummocks: mechanisms of  
1431 capitula water supply and simulated effects of evaporation. *Ecohydrology* 7, 33 – 44, 2014.

- 1432 Munir, T. M., Perkins, M., Kaing, E. and Strack, M.: Carbon dioxide flux and net primary  
1433 production of a boreal treed bog: Responses to warming and water-table-lowering simulations of  
1434 climate change, *Biogeosciences*, 12, 1091–1111, 2015.
- 1435 Murray, K. J., Harley, P. C., Beyers, J., Walz, H. and Tenhunen, J. D.: Water content effects on  
1436 photosynthetic response of Sphagnum mosses from the foothills of the Philip Smith Mountains,  
1437 Alaska, *Oecologia*, 79, 244-250, 1989.
- 1438 Nijp, J. J., Limpens, J., Metselaar, K., van der Zee, S. E. A. T. M., Berendse, F. and Robroek B. J.  
1439 M.: Can frequent precipitation moderate the impact of drought on peatmoss carbon uptake in  
1440 northern peatlands? *New Phytologist*, 203, 70-80, 2014.
- 1441 O'Neill, K. P.: Role of bryophyte-dominated ecosystems in the global carbon budget. In A. J. Shaw  
1442 and B. Goffi net [eds.] *Bryophyte biology*, 344–368, Cambridge University Press, Cambridge,  
1443 UK, 2000.
- 1444 Pastor, J., Peckham, B., Bridgham, S., Weltzin, J. and Chen J.: Plant community dynamics, nutrient  
1445 cycling, and alternative stable equilibria in peatlands. *American Naturalist*, 160, 553-568, 2002.
- 1446 Päivänen, J.: Hydraulic conductivity and water retention in peat soils, *Acta Forestalia Fennica*,  
1447 129, 1-69, 1973.
- 1448 Pouliot, R., Rochefort, L., Karofeld, E., Mercier, C. (2011) Initiation of Sphagnum moss  
1449 hummocks in bogs and the presence of vascular plants: Is there a link? *Acta Oecologica*, 37, 346-  
1450 354.
- 1451 Price, J. S., Whittington, P. N., Elrick, D. E., Strack, M., Brunet, N. and Faux, E.: A method to  
1452 determine unsaturated hydraulic conductivity in living and undecomposed moss, *Soil Sci. Soc.*  
1453 *Am. J.*, 72, 487 – 491, 2008.
- 1454 Price, J. S. and Whittington, P. N.: Water flow in Sphagnum hummocks: Mesocosm measurements  
1455 and modelling, *Journal of Hydrology* 381, 333 – 340, 2010.
- 1456 Rice, S. K., Aclander, L. and Hanson, D. T.: Do bryophyte shoot systems function like vascular  
1457 plant leaves or canopies? Functional trait relationships in Sphagnum mosses (Sphagnaceae),  
1458 *American Journal of Botany*, 95, 1366-1374, 2008.
- 1459 Riutta, T., Laine, J., Aurela, M., Rinne, J., Vesala, T., Laurila, T., Haapanala, S., Pihlatie, M. and  
1460 Tuittila, E.-S.: Spatial variation in plant community functions regulates carbon gas dynamics in a  
1461 boreal fen ecosystem, *Tellus*, 59B, 838-852, 2007.
- 1462 Robroek, B. J.M., Limpens, J., Breeuwer, A., Crushell, P. H. and Schouten, M. G.C.: Interspecific  
1463 competition between Sphagnum mosses at different water tables, *Functional Ecology*, 21, 805 –  
1464 812, 2007a.
- 1465 Robroek, B. J.M., Limpens, J., Breeuwer, A., van Ruijven, J. and Schouten, M. G.C.: Precipitation  
1466 determines the persistence of hollow Sphagnum species on hummocks, *Wetlands*, 4, 979 – 986,

1467 2007b.

1468 Robroek, B. J.M., Schouten, M. G.C., Limpens, J., Berendse, F. and Poorter, H.: Interactive effects  
1469 of water table and precipitation on net CO<sub>2</sub> assimilation of three co-occurring Sphagnum mosses  
1470 differing in distribution above the water table, *Global Change Biology* 15, 680 – 691, 2009.

1471 Ruder, S.: An overview of gradient descent optimization algorithms, CoRR, abs/1609.04747,  
1472 2016.

1473 Runkle, B.R.K., Wille, C., Gažovič M., Wilmking, M. and Kutzbach, L.: The surface energy  
1474 balance and its drivers in a boreal peatland fen of northwestern Russia, *Journal of Hydrology*, 511,  
1475 359-373, 2014.

1476 [Rydin, H.: Interspecific competition between Sphagnum mosses on a raised bog. \*Oikos\*, 413-423,  
1477 1993.](#)

1478 [Rydin, H.: Competition and niche separation in Sphagnum. \*Canadian Journal of Botany\*, 64\(8\),  
1479 1817-1824, 1986.](#)

1480 [Rydin, H.: Competition between Sphagnum species under controlled conditions. \*Bryologist\*, 302-  
1481 307, 1997.](#)

1482 Rydin, H. and McDonald A. J. S.: Tolerance of Sphagnum to water level. *Journal of Bryology*, 13,  
1483 571–578, 1985.

1484 Rydin, H., Gunnarsson, U., and Sundberg, S.: The role of Sphagnum in peatland development and  
1485 persistence, in: *Boreal peatland ecosystems*, edited by: Wieder, R. K., and Vitt, D. H., 30  
1486 *Ecological Studies Series*, Springer Verlag, Berlin, 47–65, 2006.

1487 Sato, H., Itoh, A. and Kohyama, T.: SEIB-DGVM: A new Dynamic Global Vegetation Model  
1488 using a spatially explicit individual-based approach, *Ecol. Model.*, 200, 279–307, 2007.

1489 Scheiter, S., Langan, L. and Higgins, S. I.: Next-generation dynamic global vegetation models:  
1490 learning from community ecology, *New Phytologist*, 198, 957-969, 2013.

1491 Schipperges, B. and Rydin, H.: Response of photosynthesis of Sphagnum species from contrasting  
1492 microhabitats to tissue water content and repeated desiccation, *The New Phytologist*, 140, 677-  
1493 684, 1998.

1494 Silvola, J., Aaltonen, H. (1984) Water content and photo- synthesis in the peat mosses Sphagnum  
1495 fuscum and S. angustifolium. *Annales Botanici Fennici* 21, 1–6.

1496 Smirnov, N.: The carbohydrates of bryophytes in relation to desiccation tolerance, *Journal of*  
1497 *Bryology*, 17, 185-19, 1992.

1498 Straková, P., Niemi, R. M., Freeman, C., Peltoniemi, K., Toberman, H., Heiskanen, I., Fritze, H.  
1499 and Laiho, R.: Litter type affects the activity of aerobic decomposers in a boreal peatland more



1500 than site nutrient and water table regimes, *Biogeosciences*, 8, 2741-2755, 2011.

1501 Straková, P., Penttilä, T., Laine, J., and Laiho, R.: Disentangling direct and indirect effects of water  
1502 table drawdown on above- and belowground plant litter decomposition: consequences for  
1503 accumulation of organic matter in boreal peatlands. *Global Change Biology*, 18, 322-335, 2012.

1504 Strandman, H., Väisänen, H. and Kellomäki, S.: A procedure for generating synthetic weather  
1505 records in conjunction of climatic scenario for modelling of ecological impacts of changing climate  
1506 in boreal conditions, *Ecol. Model.*, 70, 195–220, 1993.

1507 Szurdoki, E., Márton, O., Szövényi, P. ~~(2014)~~: Genetic and morphological diversity of *Sphagnum*  
1508 *angustifolium*, *S. flexuosum* and *S. fallax* in Europe. *Taxon*, 63, 237–48, 2014.

1509 Tahvanainen, T.: Abrupt ombrotrophication of a boreal aapa mire triggered by hydrological  
1510 disturbance in the catchment, *Journal of Ecology*, 99, 404-415, 2011.

1511 Tatsumi, S., Cadotte M. W. and Mori, A. S.: Individual-based models of community assembly:  
1512 Neighbourhood competition drives phylogenetic community structure, *J. Ecol.*, 107, 735–746,  
1513 2019.

1514 Thompson, D. K., Baisley, A. S. and Waddington, J. M.: Seasonal variation in albedo and radiation  
1515 exchange between a burned and unburned forested peatland: implications for peatland evaporation,  
1516 *Hydrological Processes*, 29, 3227-3235, 2015.

1517

1518 [Titus, J. E., and Wagner, D. J.: Carbon balance for two Sphagnum mosses: water balance](#)  
1519 [resolves a physiological paradox. \*Ecology\*, 65\(6\), 1765-1774, 1984.](#)

1520

1521 Turetsky, M. R.: The role of bryophytes in carbon and nitrogen cycling, *Bryologist*, 106, 395 –  
1522 409, 2003.

1523 Turetsky, M. R., Crow, S. E., Evans, R. J., Vitt, D. H. and Wieder, R. K.: Trade-offs in resource  
1524 allocation among moss species control decomposition in boreal peatlands, *Journal of Ecology*, 96,  
1525 1297-1305, 2008.

1526 Turetsky, M. R., Bond-Lamberty, B., Euskirchen, E., Talbot, J., Frolking, S., McGuire, A. D. and  
1527 Tuittila, E.: The resilience and functional role of moss in boreal and arctic ecosystems, *New*  
1528 *Phytologist*, 196, 49-67, 2012.

1529 van Gaalen, K. E., Flanagan, L. B., Peddle, D. R.: Photosynthesis, chlorophyll fluorescence and  
1530 spectral reflectance in *Sphagnum* moss at varying water contents. *Oecologia*, 153, 19 – 28, 2007.

1531 van Genuchten, M.: A closed-form equation for predicting the hydraulic conductivity of  
1532 unsaturated soils, *Soil Science Society of American Journal*, 44, 892–898, 1980.

1533 Väiliranta, M., Korhola, A., Seppä, H., Tuittila, E. S., Sarmaja-Korjonen, K., Laine, J. and Alm, J.:



1534 High-resolution reconstruction of wetness dynamics in a southern boreal raised bog, Finland,  
1535 during the late Holocene: a quantitative approach, *The Holocene*, 17, 1093–1107, 2007.

1536 Venäläinen, A., Tuomenvirta, H., Lahtinen, R. and Heikinheimo, M.: The influence of climate  
1537 warming on soil frost on snow-free surfaces in Finland, *Climate Change*, 50, 111-128, 2001.

1538 Vionnet, V., Brun, E., Morin, S., Boone, A., Faroux, S., Le Moigne, P., Martin, E. and Willemet,  
1539 J.-M.: The detailed snowpack scheme Crocus and its implementation in SURFEX v7.2,  
1540 *Geoscientific Model Development*, 5, 773-791, 2012

1541 Vitt, D. H.: Peatlands: Ecosystems dominated by bryophytes. In A. J. Shaw and B. Goffi net  
1542 [eds.], *Bryophyte biology*, 312 – 343, Cambridge University Press, Cambridge, UK, 2000.

1543 Waddington, J. M., Morris, P. J., Kettridge, N., Granath, G., Thompson, D. K. and Moore, P. A.:  
1544 Hydrological feedbacks in northern peatlands, *Ecohydrology*, 8, 113 – 127, 2015.

1545 Wania, R., Ross, I. and Prentice, I. C.: Integrating peatlands and permafrost into a dynamic global  
1546 vegetation model: 2. Evaluation and sensitivity of vegetation and carbon cycle processes, *Global*  
1547 *Biogeochemical Cycles*, 23, GB3015, DOI:10.1029/2008GB003413, 2009.

1548 Weiss, R., Alm, J., Laiho, R. and Laine, J.: Modeling moisture retention in peat soils, *Soil Science*  
1549 *Society of America Journal*, 62, 305–313, 1998.

1550 Whittington, P. N. and Price, J. S.: The effects of water table draw-down (as a surrogate for  
1551 climate change) on the hydrology of a fen peatland, Canada, *Hydrological Processes*, 20, 3589–  
1552 3600, 2006.

1553 Wilson, P. G.: The relationship among micro-topographic variation, water table depth and  
1554 biogeochemistry in an ombrotrophic bog, Master Thesis, Department of Geography McGill  
1555 University, Montreal, Quebec, p. 103, 2012.

1556 Wojtuń B., Sendyk A. and Martynia, D.: Sphagnum species along environmental gradients in  
1557 mires of the Sudety Mountains (SW Poland), *Boreal Environment Research*, 18, 74–88, 2003.

1558 Wu, J. and Roulet, N. T.: Climate change reduces the capacity of northern peatlands to absorb the  
1559 atmospheric carbon dioxide: The different responses of bogs and fens. *Global Biogeochemical*  
1560 *Cycles*, doi.org/10.1002/2014GB004845, 2014.

1561 Wullschleger, S. D., Epstein, H. E., Box, E. O., Euskirchen, E. S., Goswami, S., Iversen, C. M.,  
1562 Kattge, J., Norby, R. J., van Bodegom, P. M. and Xu, X.: Plant functional types in Earth system  
1563 models: past experiences and future directions for application of dynamic vegetation models in  
1564 high-latitude ecosystems, *Ann. Bot.*, 114, 1–16, 2014.

1565



<u>Symbol</u>	<u>Description</u>	<u>Unit</u>
<u>A</u>	<u>Net photosynthesis rate</u>	<u><math>\mu\text{mol m}^{-2} \text{s}^{-1}</math></u>
<u>A<sub>m</sub></u>	<u>Maximal net photosynthesis rate</u>	<u><math>\mu\text{mol m}^{-2} \text{s}^{-1}</math></u>
<u><math>\alpha_{imm}</math></u>	<u>Temperature constant for NSC immobilization</u>	
<u><math>\alpha_{PPFD}</math></u>	<u>Half-saturation point of PPFD for photosynthesis.</u>	<u><math>\mu\text{mol m}^{-2} \text{s}^{-1}</math></u>
<u>B<sub>cap</sub></u>	<u>Capitulum biomass</u>	<u><math>\text{g m}^{-2}</math></u>
<u>C<sub>T</sub></u>	<u>Specific heat</u>	<u><math>\text{J K}^{-1} \text{kg}^{-1}</math></u>
<u>D<sub>S</sub></u>	<u>Capitulum density</u>	<u>shoots <math>\text{cm}^{-2}</math></u>
<u>dH</u>	<u>Annual height growth of <i>Sphagnum</i> mosses</u>	<u>cm</u>
<u>dWT</u>	<u>Hummock-lawn differences in water table</u>	<u>cm</u>
<u>E</u>	<u>Rate of evaporation</u>	<u>cm timestep<sup>-1</sup></u>
<u>f<sub>w</sub></u>	<u>Water content multiplier on photosynthesis rate</u>	
<u>f<sub>T</sub></u>	<u>Temperature multiplier on photosynthesis rate</u>	
<u>h</u>	<u>Water potential</u>	<u>cm</u>
<u>H<sub>c</sub></u>	<u>Shoot height of <i>Sphagnum</i> mosses</u>	<u>cm</u>
<u>H<sub>cap</sub></u>	<u>Height of capitula</u>	<u>cm</u>
<u>H<sub>spc</sub></u>	<u>Biomass density of living <i>Sphagnum</i> stems</u>	<u><math>\text{g m}^{-2} \text{cm}^{-1}</math></u>
<u>I</u>	<u>Rate of net inflow water</u>	<u>cm</u>
<u>k<sub>imm</sub></u>	<u>Specific immobilization rate</u>	<u><math>\text{g g}^{-1}</math></u>
<u>JD<sub>thaw</sub></u>	<u>Julian day when thawing completed</u>	
<u>K<sub>h</sub></u>	<u>Hydraulic conductivity of peat layer</u>	<u><math>\text{cm s}^{-1}</math></u>
<u>K<sub>m</sub></u>	<u>Hydraulic conductivity of moss layer</u>	<u><math>\text{cm s}^{-1}</math></u>
<u>K<sub>sat</sub></u>	<u>Saturated hydraulic conductivity</u>	<u><math>\text{cm s}^{-1}</math></u>

<u><math>K_T</math></u>	<u>Thermal conductivity</u>	<u><math>W m^{-1} K^{-1}</math></u>
<u><math>l_c</math></u>	<u>Width of a grid cell in simulation</u>	<u>cm</u>
<u><math>M_B</math></u>	<u>Immobilized NSC to biomass production</u>	<u>g</u>
<u><math>NSC_{max}</math></u>	<u>Maximal NSC concentration in <i>Sphagnum</i> biomass</u>	<u><math>g g^{-1}</math></u>
<u><math>P</math></u>	<u>Precipitation</u>	<u>cm</u>
<u><math>Pm</math></u>	<u>Mass-based rate of maximal gross photosynthesis</u>	<u><math>\mu mol g^{-1} s^{-1}</math></u>
<u><math>PPFD</math></u>	<u>Photosynthetic photon flux density</u>	<u><math>\mu mol m^{-2} s^{-1}</math></u>
<u><math>\rho_{bulk}</math></u>	<u>Bulk density of peat</u>	<u><math>g cm^{-3}</math></u>
<u><math>r_{aero}</math></u>	<u>Aerodynamic resistance</u>	<u><math>s m^{-1}</math></u>
<u><math>r_{bulk}</math></u>	<u>Cell-level bulk surface resistance</u>	<u><math>s m^{-1}</math></u>
<u><math>r_{ss}</math></u>	<u>Bulk surface resistance of community</u>	<u><math>s m^{-1}</math></u>
<u><math>Rh</math></u>	<u>Relative humidity</u>	<u>%</u>
<u><math>Rs</math></u>	<u>Mass-based respiration rate</u>	<u><math>\mu mol g^{-1} s^{-1}</math></u>
<u><math>R_s</math></u>	<u>Incoming shortwave radiation</u>	<u><math>W m^{-2}</math></u>
<u><math>R_l</math></u>	<u>Incoming longwave radiation</u>	<u><math>W m^{-2}</math></u>
<u><math>S_c</math></u>	<u>Area of a cell in model simulation</u>	<u><math>m^2</math></u>
<u><math>S_{imm}</math></u>	<u>Multiplier for temperature threshold</u>	
<u><math>Sv_i</math></u>	<u>Evaporative area of a cell <math>i</math></u>	<u><math>cm^2</math></u>
<u><math>T</math></u>	<u>Capitulum temperature</u>	<u><math>^{\circ}C</math></u>
<u><math>T_a</math></u>	<u>Air temperature</u>	<u><math>^{\circ}C</math></u>
<u><math>T_{opt}</math></u>	<u>reference temperature of respiration (20 <math>^{\circ}C</math>)</u>	<u><math>^{\circ}C</math></u>
<u><math>u</math></u>	<u>Wind speed</u>	<u><math>m s^{-1}</math></u>
<u><math>W_{cap}</math></u>	<u>Capitulum water content</u>	<u><math>g g^{-1}</math></u>

<u><math>W_{cmp}</math></u>	<u>Capitulum water content at the compensation point</u>	<u><math>g\ g^{-1}</math></u>
<u><math>W_{max}</math></u>	<u>Maximum water content of capitula</u>	<u><math>g\ g^{-1}</math></u>
<u><math>W_{opt}</math></u>	<u>Optimal capitulum water content for photosynthesis</u>	<u><math>g\ g^{-1}</math></u>
<u><math>W_{cf}</math></u>	<u>field-water contents of <i>Sphagnum</i> capitulum</u>	<u><math>g\ g^{-1}</math></u>
<u><math>W_{sf}</math></u>	<u>field-water contents of <i>Sphagnum</i> stem</u>	<u><math>g\ g^{-1}</math></u>
<u><math>WT_m</math></u>	<u>Measured multi-year mean of weekly water table</u>	<u>cm</u>
<u><math>WT_s</math></u>	<u>Simulated multi-year mean of weekly water table</u>	<u>cm</u>
<u><math>z_m</math></u>	<u>Thickness of the living moss layer</u>	<u>cm</u>
<u><math>\theta_m</math></u>	<u>Volumetric water content of moss layer</u>	
<u><math>\theta_r</math></u>	<u>permanent wilting point water content</u>	
<u><math>\theta_s</math></u>	<u>saturated water content</u>	
<u>Abbreviations:</u>		
<u><math>\Gamma</math></u>	<u>Learning rate of gradient descent algorithms</u>	
<u>D-layer</u>	<u>Daily-based snow layer</u>	
<u>ICOS</u>	<u>Integrated Carbon Observation System</u>	
<u>JD</u>	<u>Julian day</u>	
<u>NSC</u>	<u>Nonstructural carbon</u>	
<u>PMS</u>	<u>Peatland Moss Simulator</u>	
<u>RWC</u>	<u>Capitulum water ?? row 286</u>	
<u>SD</u>	<u>Standard deviation</u>	
<u>SE</u>	<u>Standard error</u>	
<u>SSE</u>	<u>Sum of squared error</u>	
<u>SVAT</u>	<u>Soil-vegetation-atmosphere transport</u>	

---

WT

Water table

---

1567

1568

1569 Table. 1–2 Species-specific values of morphological and photosynthetic parameters for *S.*  
 1570 *magellanicum* and *S. fallax*. The parameters include: capitulum density ( $D_s$ , ~~capitula cm<sup>-2</sup>~~),  
 1571 capitulum biomass ( $B_{cap}$ , ~~g m<sup>-2</sup>~~), specific height of stem ( $H_{spc}$ , ~~cm g<sup>-1</sup> m<sup>-2</sup>~~), maximal gross  
 1572 photosynthesis rate at 20 °C ( $Pm_{20}$ , ~~μmol g<sup>-1</sup> s<sup>-1</sup>~~), respiration rate at 20 °C ( $Rs_{20}$ ), half-saturation  
 1573 point of photosynthesis ( $\alpha_{PPFD}$ , ~~μmol g<sup>-1</sup> s<sup>-1</sup>~~), and polynomial coefficients ( $a_{w0}$ ,  $a_{w1}$  and  $a_{w2}$ ) for  
 1574 the responses of net photosynthesis to capitulum water content. Parameter values are given as  
 1575 (mean ± standard deviation).  
 1576

Parameter	Unit	<i>S. magellanicum</i>	<i>S. fallax</i>	Equation
$D_s$	cm <sup>-2</sup>	0.922±0.289	1.46±0.323	- <sup>a</sup>
$B_{cap}$	g m <sup>-2</sup>	75.4±21.5	69.2±19.6	- <sup>a</sup>
$H_{spc}$	g <sup>-1</sup> cm <sup>-1</sup>	45.4 ± 7.64	32.6±6.97	(7)
$Pm_{20}$	$\frac{\mu\text{mol g}^{-1}}{\text{s}^{-1}}$	0.0189±0.00420	0.0140±0.00212	(2)
$Rs_{20}$	$\frac{\mu\text{mol g}^{-1}}{\text{s}^{-1}}$	0.00729±0.00352	0.00651±0.00236	(2)
$\alpha_{PPFD}$	$\frac{\mu\text{mol m}^{-2}}{\text{s}^{-1}}$	101.4±14.1	143±51.2	(2)
$a_{w0}$	unitless	-1.354±0.623	-1.046±0.129	(4)
$a_{w1}$	unitless	0.431±0.197	0.755±0.128	(4)
$a_{w2}$	unitless	-0.0194±0.0119	-0.0751±0.0223	(4)

1577 <sup>a</sup> the parameter was used in the linear models predicting the log<sub>10</sub>-transformed capitulum water  
 1578 potential ( $h$ ) and bulk resistance ( $r_{bulk}$ ) for *S. fallax* and *S. magellanicum*. ~~The function is detailed~~  
 1579 ~~in Table 2 and Table 3 in Gong et al. (2019).~~ The capitulum density and photosynthetic  
 1580 parameter values measured here are well within the range of those reported in literature for these  
 1581 species (McCarter & Price, 2014; Laing et al. 2014; Bengtsson et al. 2016; Korrensalo et al.  
 1582 2016).  
 1583  
 1584  
 1585



1586 Table- 23. Parameters values for SVAT simulations (Module III). The parameters include:  
 1587 saturated hydraulic conductivity ( $K_{sat}$ ), water retention parameters of water retention curves ( $\alpha$  and  
 1588  $n$ ), saturated water content ( $\theta_s$ ), permanent wilting point water content ( $\theta_r$ ), snow layer surface albedos  
 1589 ( $a_s$ ,  $a_l$ ), the thermal conductivity ( $K_T$ ), specific heat ( $C_T$ ), maximal nonstructural carbon (NSC)  
 1590 concentration ( $NSC_{max}$ ).

Parameter	Value	Equation	Source
$K_{sat}$	162	A6	McCarter and Price, 2014
$n$	1.43	A5	McCarter and Price, 2014
$\alpha$	2.66	A5	McCarter and Price, 2014
$\theta_s$	0.95 <sup>a</sup>	A5	Päivänen, 1973
$\theta_r$	0.071 <sup>b</sup>	A5	Weiss et al., 1998
$a_s$	0.15	A9	Runkle et al., 2014
$a_l$	0.02	A10	Thompson et al., 2015
$K_{T,water}$	0.57	A4	Letts et al., 2000
$K_{T,ice}$	2.20	A4	Letts et al., 2000
$K_{T,org}$	0.25	A4	Letts et al., 2000
$C_{T,water}$	4.18	A3	Letts et al., 2000
$C_{T,ice}$	2.10	A3	Letts et al., 2000
$C_{T,org}$	1.92	A3	Letts et al., 2000
$NSC_{max}$	0.045	6	Turetsky et al., 2008

1591 <sup>a</sup> The value was calculated from bulk density ( $\rho_{bulk}$ ) as  $\theta_s = 97.95 - 79.72\rho_{bulk}$  following Päivänen  
 1592 (1973); <sup>b</sup> The value was calculated as  $\theta_r = 4.3 + 67\rho_{bulk}$  following Weiss et al. (1998).

1593 Table- 34. Results from the Test 2test addressing the robustness of the model to the uncertainties  
1594 in a set of parameters. Each parameter was increased or decreased by 10%. Model was run for *S.*  
1595 *magellanicum* and *S. fallax* in their preferential habitats. Difference in mean cover between  
1596 simulations under changed and unchanged parameter values are given with the standard deviations  
1597 (SD) of the means in brackets. The parameters include: specific immobilization rate (*kimm*),  
1598 maximal nonstructural carbon (NSC) concentration (*NSC<sub>max</sub>*), hydraulic conductivity of moss layer  
1599 (*K<sub>m</sub>*), hydraulic conductivity of peat layer (*K<sub>h</sub>*), water retention parameters of water retention curves  
1600 (*α* and *n*), snow layer surface albedo (*a<sub>s</sub>*) and aerodynamic resistance (*r<sub>aero</sub>*).

Change in parameter value	Equation	Changes in simulated cover, % (SD)	
		<i>S. magellanicum</i> (hummock)	<i>S. fallax</i> (lawn)
<i>kimm</i> +10%	5	-1.2 (3.5)	-3.5 (3.8)
<i>kimm</i> -10%		+2.7 (0.4)	-5.0 (3.4)
<i>NSC<sub>max</sub></i> +10%	6	+4.5 (2.9)	+0.7 (3.0)
<i>NSC<sub>max</sub></i> -10%		-0.7 (4.0)	-4.8 (4.5)
<i>K<sub>m</sub></i> +10%	10	+1.0 (3.1)	-1.7 (2.3)
<i>K<sub>m</sub></i> -10%		-1.7 (2.7)	+4.1 (4.3)
<i>K<sub>h</sub></i> +10%	A1	-1.1 (3.0)	+1.1 (2.0)
<i>K<sub>h</sub></i> -10%		-1.8 (3.1)	-0.5 (2.7)
<i>n</i> +10%	A5	-1.6 (3.2)	-3.2 (3.2)
<i>n</i> -10%		-9.4 (3.6)	-0.3 (2.9)
<i>α</i> +10 %	A5	-0.5 (2.9)	-0.3 (2.3)
<i>α</i> -10 %		-1.3 (3.6)	+3.2 (1.0)
<i>a<sub>s</sub></i> +10%	A9	-2.2 (3.8)	+0.6 (2.1)
<i>a<sub>s</sub></i> -10%		+3.3 (3.4)	+1.2 (1.8)
<i>r<sub>aero</sub></i> +10%	A14, A15	-2.1 (3.4)	+0.3 (2.1)
<i>r<sub>aero</sub></i> -10%		-3.8 (4.4)	+2.3 (1.1)

## 1602 Appendix A. Calculating community SVAT scheme (Module III)

### 1603 *Transport of water and heat in peat profile*

1604 Simulating the transport of water and heat in the peat profiles was based on Gong et al. (2012, 2013). Here  
1605 we list the key algorithms and parameters. Ordinary differential equations governing the vertical transport  
1606 of water and heat in peat profiles were given as:

$$1607 \quad C_h \frac{\partial h}{\partial t} = \frac{\partial}{\partial z} \left[ K_h \left( \frac{\partial h}{\partial z} + 1 \right) \right] + S_h \quad (A1)$$

$$1608 \quad C_T \frac{\partial T}{\partial t} = \frac{\partial}{\partial z} \left( K_T \frac{\partial T}{\partial z} \right) + S_T \quad (A2)$$

1609 where  $t$  is the time step;  $z$  is the thickness of peat layer;  $h$  is the water potential;  $T$  is the temperature;  $C_h$  and  
1610  $C_T$  are the specific capacity of water (i.e.  $\partial\theta/\partial h$ ) and heat;  $K_h$  and  $K_T$  are the hydraulic conductivity and  
1611 thermal conductivity, respectively; and  $S_h$  and  $S_T$  are the sink terms for water and energy, respectively.

1612  $C_T$  and  $K_T$  were calculated as the volume-weighted sums from components of water, ice and organic  
1613 matter:

$$1614 \quad C_T = C_{water}\theta_{water} + C_{ice}\theta_{ice} + C_{org}(1 - \theta_{water} - \theta_{ice}) \quad (A3)$$

$$1615 \quad K_T = K_{water}\theta_{water} + K_{ice}\theta_{ice} + K_{org}(1 - \theta_{water} - \theta_{ice}) \quad (A4)$$

1616 where  $C_{water}$ ,  $C_{ice}$  and  $C_{org}$  are the specific heats of water, ice and organic matter, respectively;  $K_{water}$ ,  $K_{ice}$   
1617 and  $K_{org}$  are the thermal conductivities of water, ice and organic matter, respectively; and  $\theta_{water}$  and  $\theta_{ice}$  are  
1618 the volumetric contents of water and ice, respectively.

1619 For a given  $h$ ,  $C_h = \partial\theta(h)/\partial h$  was derived from the van Genuchten water retention model (van Genuchten,  
1620 1980) as:

$$1621 \quad \theta(h) = \theta_r + \frac{(\theta_s - \theta_r)}{[1 + (\alpha|h^n|)^m]} \quad (A5)$$

1622 where  $\theta_s$  is the saturated water content;  $\theta_r$  is the permanent wilting point water content;  $\alpha$  is a scale parameter  
1623 inversely proportional to mean pore diameter;  $n$  is a shape parameter; and  $m=1-1/n$ .

1624 Hydraulic conductivity ( $K_h$ ) in an unsaturated peat layer was calculated as a function of  $\theta$  by combining  
1625 the van Genuchten model with the Mualem model (Mualem, 1976):

$$1626 \quad K_h(\theta) = K_{sat} S_e^{L_e} \left[ 1 - \left( 1 - S_e^{1/m} \right)^m \right] \quad (A6)$$

1627 where  $K_{sat}$  is the saturated hydraulic conductivity;  $S_e$  is the saturation ratio and  $S_e = (\theta - \theta_r)/(\theta_s - \theta_r)$ ; and  $L_e$  is  
1628 the shape parameter ( $L_e=0.5$ ; Mualem, 1976).

1629

### 1630 *Boundary conditions and surface energy balance*

1631 A zero-flow condition was assumed at the lower boundary of the peat column. The upper boundary  
1632 condition was defined by the surface energy balance, which was driven by net radiation ( $Rn$ ). The dynamics  
1633 of  $Rn$  at surface  $x$  ( $x=0$  for vascular canopy and  $x=1$  for moss surface) was determined by the balance

1634 between incoming and outgoing radiation components:

$$1635 \quad Rn_x = Rsn_{b,x} + Rsn_{d,x} + Rln_x \quad (A7)$$

1636 where  $Rsn_{b,x}$  and  $Rsn_{d,x}$  are the absorbed energy from direct and diffuse radiation;  $Rln_x$  is the absorbed net  
1637 longwave radiation.

1638 Algorithms for calculating the net radiation components were detailed in Gong et al. (2013), as modified  
1639 from the methods of Chen et al. (1999). Canopy light interception was determined by the light-extinction  
1640 coefficient ( $k_{light}$ ), leaf area index ( $Lc$ ) and solar zenith angle. The partitioning of reflected and absorbed  
1641 irradiances at ground surface was regulated by the surface albedos for the shortwave ( $a_s$ ) and longwave ( $a_l$ )  
1642 components, and the temperature of surface  $x$  ( $T_x$ ) also affects net longwave radiation:

$$1643 \quad Rn_x = Rsn_{b,x} + Rsn_{d,x} + Rln_x \quad (A8)$$

$$1644 \quad Rsn_{d,x} = Rsid,x(1 - a_s) \quad (A9)$$

$$1645 \quad Rln_x = Rli,x(1 - a_l) - \varepsilon\delta T_x^4 \quad (A10)$$

1646 where  $Rsi_b$ ,  $Rsid$ ,  $Rli$  are the incoming beam, diffusive and longwave radiations;  $\varepsilon$  is the emissivity ( $\varepsilon = 1 -$   
1647  $a_l$ );  $\delta$  is the Stefan Boltzmann's constant ( $5.67 \times 10^{-8} \text{ W m}^{-2} \text{ K}^{-4}$ ).

1648  $Rn_x$  was partitioned into latent heat flux ( $\lambda E_x$ ), sensible heat flux ( $H_x$ ) and ground heat flux (for canopy  
1649  $G_I=0$ ):

$$1650 \quad Rn_x = H_x + \lambda E_x + G_x \quad (A11)$$

$$1651 \quad G_1 = K_T (T_x - Ts)/(0.5z) \quad (A12)$$

1652 where  $Ts$  is the temperature of the moss carpet;  $z$  is the thickness of the moss layer ( $z = 5 \text{ cm}$ ).

1653 The latent heat flux was calculated by the “interactive scheme” (Daamen and McNaughton, 2000; see  
1654 also in Gong et al., 2016), which is a K-theory-based, multi-source model:

$$1655 \quad \lambda E_x = \frac{(\Delta/\gamma)A_x r_{sa,x} + \lambda VPD_b}{r_{b,x} + (\Delta/\gamma)r_{sa,x}} \quad (A13)$$

1656 where  $\Delta$  is the slope of the saturated vapor pressure curve against air temperature;  $\lambda$  is the latent heat of  
1657 vaporization;  $E$  is the evaporation rate;  $VPD_b$  is the vapor pressure deficit at  $z_b$ ;  $r_{b,x}$  is the total resistance to  
1658 water vapor flow, the sum of boundary layer resistance ( $r_{sa,x}$ ) and surface resistance ( $r_{ss}$ ); and  $A$  is the  
1659 available energy for evapotranspiration and  $A_x = Rn_x - G_x$ .

1660 The calculations of  $\gamma$ ,  $\lambda$  and  $VPD_b$  require the temperature ( $T_b$ ) and vapor pressure ( $e_b$ ) at the mean source  
1661 height ( $z_b$ ). These variables were related to the total of latent heat ( $\sum \lambda E_x$ ) and sensible heat ( $\sum H_x$ ) from all  
1662 surfaces using the Penman-type equations:

$$1663 \quad \Sigma \lambda E_x = \rho_a C_p (e_b - e_a)/(r_{aero} \gamma) \quad (A14)$$

$$1664 \quad \Sigma H_x = \rho_a C_p (T_b - T_a)/r_{aero} \quad (A15)$$

1665 where  $\rho_a C_p$  is the volumetric specific heat of air;  $r_{aero}$  is the aerodynamic resistance between  $z_b$  and the

1666 reference height  $z_a$ , and was a function of  $T_b$  accounting for the atmospheric stability (Choudhury and  
1667 Monteith, 1988); and  $\gamma$  is the psychrometric constant ( $\gamma = \rho_a C_p / \lambda$ ).

1668 Changes in the energy balance affect the surface temperature ( $T_x$ ) and vapor pressure ( $e_x$ ), which further  
1669 feed back to the energy availability (Eq. A10, A12), the source-height temperature,  $VPD$  and the resistance  
1670 parameters (e.g.,  $r_{aero}$ ). The values of  $T_x$  and  $e_x$  were solved iteratively by coupling the energy balance  
1671 equations (eqs. A11–A15) with the Penman-type equations (see also Appendix B in Gong et al., 2016):

$$1672 \lambda E_x = \rho_a C_p (e_x - e_b) / (r_{sa,x} \gamma) \quad (A16)$$

$$1673 H_x = \rho_a C_p (T_x - T_b) / r_{sa,x} \quad (A17)$$

1674 where the boundary-layer resistance for ground surface ( $r_{sa,l}$ ) and canopy ( $r_{sa,0}$ ) were calculated following  
1675 the approaches of Choudhury and Monteith (1988).

1676

1677 *Sink terms of transport functions for water and heat*

1678 The sink term  $S_{h,i}$  (see Eq. A11) for each soil layer  $i$  was calculated as:

$$1679 S_{h,i} = E_i - P_i - W_{melt,i} - I_i \quad (A18)$$

1680 where  $E_i$  is the evaporation loss of water from the layer;  $P_i$  is rainfall ( $P_i = 0$  if the layer is not topmost, i.e.  
1681  $i > 1$ );  $W_{melt,i}$  is the amount of melt water added to the layer;  $I_i$  is the net water inflow and was calibrated in  
1682 Section 2.5.

1683 The value of  $E_i$  was calculated as:

$$1684 E_i = f_{top} E_0 + f_{root}(i) E_1 \quad (A19)$$

1685 where  $E_0$  and  $E_1$  are the evaporation rate from ground surface and canopy (Eq. A13);  $f_{top}$  is the location  
1686 multiplier for the topmost layer ( $f_{top} = 0$  in cases  $i > 1$ ); and  $f_{root}(i)$  is the fraction of fine-root biomass in layer  
1687  $i$ .

1688 The value of  $W_{melt,i}$  was controlled by the freeze-thaw dynamics of soil water and snow pack, which were  
1689 related to the heat diffusion in soil profile (Eq. A2). We set the freezing point temperature to 0 °C, and the  
1690 temperature of a soil layer was held constant (0 °C) during freezing or melting. For the  $i$ th soil layer, the  
1691 sink term ( $S_T$ ) in heat transport equation (Eq. A2) was calculated as:

$$1692 S_{T,i} = f_{phase} \max(|T_i| C_{T,i} W_{phase} \lambda_{melt}) \quad (A20)$$

1693 where  $C_{T,i}$  is specific heat of soil layer (Eq. A13);  $W_{phase}$  is the water content for freezing ( $W_{phase} = \theta_w$ ) or  
1694 melting ( $W_{phase} = \theta_{ice}$ );  $\lambda_{melt}$  is the latent heat of freezing;  $f_{phase}$  is binomial coefficient that denotes the existence  
1695 of freezing or thawing. For each time step  $t$ , we computed  $T_i(t)$  with a piror assumption that  $S_{T,i} = 0$ . Then  
1696  $f_{phase}$  was determined by whether the temperature changed across the freezing point, i.e.  $f_{phase} = 1$  if  $T_i(t) * T_i(t-1) \leq 0$ , otherwise  $f_{phase} = 0$ .

1698

1699 **Appendix B. Methods and results of the empirical study on *Sphagnum capitula* water retention as a**  
1700 **controlling mechanism for peatland moss community dynamics**

1701

1702 *Measurement of morphological traits*

1703 To quantify morphological traits, samples of *S. fallax* and *S. magellanicum* were collected at the end of  
1704 August 2016 with a core (size d 7cm, area 50 cm<sup>2</sup>, height at least 8 cm) maintaining the natural density of  
1705 the stand. Samples were stored in plastic bags at cool room (4 °C) until measurements. Eight replicates were  
1706 collected for each species. For each sample, capitulum density ( $D_s$ , shoots cm<sup>-2</sup>) was measured and ten moss  
1707 shoots were randomly selected and separated into capitula and stems (5 cm below capitula). The capitula  
1708 and stems were moistened and placed on top of a tissue paper for 2 minutes to extract free-moving water,  
1709 before weighing them for water-filled fresh weight. The samples were dried at 60 °C for at least 48h to  
1710 measure the dry masses. The field-water contents of capitula ( $W_{cf}$ , g g<sup>-1</sup>) and stems ( $W_{sf}$ , g g<sup>-1</sup>) were then  
1711 calculated as the ratio of water to dry mass for each sample. The biomass of capitula ( $B_{cap}$ , g m<sup>-2</sup>) and living  
1712 stems ( $B_{st}$ , g m<sup>-2</sup>) were calculated by multiplying the dry masses with the capitulum density ( $D_s$ ). Biomass  
1713 density of living stems ( $H_{spc}$ , g cm<sup>-1</sup> m<sup>-2</sup>) was calculated by dividing  $B_{st}$  with the length of stems.

1714 *Measurement of photosynthetic traits*

1715 We measured the photosynthetic light response curves for *S. fallax* and *S. magellanicum* with fully  
1716 controlled, flow-through gas-exchange fluorescence measurement systems (GFS-3000, Walz, Germany;  
1717 Li-6400, Li-Cor, US) under varying light levels. In 2016, measurements on field-collected samples were  
1718 done during May and early June, which is a peak growth period for *Sphagna* (Korrensalo et al. 2017).  
1719 Samples were collected from the field site each morning and were measured the same day at Hyytiälä field  
1720 station. Samples were stored in plastic containers and moistened with peatland water to avoid changes in  
1721 plant status during the measurement. Right before the measurement we separated *Sphagnum* capitula from  
1722 their stems and dried them lightly using tissue paper before placing [an even layer of](#) them in a custom-made  
1723 cuvette [by retaining the same density as naturally at field](#) (Korrensalo et al. 2017). Net photosynthesis rate  
1724 ( $A$ , μmol m<sup>-2</sup> s<sup>-1</sup>) was measured at 1500, 250, 35, and 0 μmol m<sup>-2</sup> s<sup>-1</sup> photosynthetic photon flux density  
1725 (PPFD). [The light levels were chosen based on previous investigation by Laine et al. \(2011, 2015\), which](#)  
1726 [showed increasing A until PPFD at 1500 and no photoinhibition even at high values of 2000 μmol m<sup>-2</sup> s<sup>-1</sup>.](#)  
1727 The samples were allowed to adjust to cuvette conditions before the first measurement and after each change  
1728 in the PPFD level until the CO<sub>2</sub> rate had reached a steady level, otherwise the cuvette conditions were kept  
1729 constant (temperature 20°C, CO<sub>2</sub> concentration 400 ppm, ~~relative humidity of inflow air 60%~~, flow rate  
1730 500 μmol s<sup>-1</sup>, ~~and~~ impeller at level 5 ~~and relative humidity of inflow air 60%~~, ~~yet the relative humidity~~  
1731 [remained on average 81% during the measurements](#)). The time required for a full measurement cycle varied  
1732 between 60 and 120 minutes. Each sample was weighed before and after the gas-exchange measurement,  
1733 then dried at 40°C for 48 h to determine the biomass of capitula ( $B_{cap}$ ). For each species, four samples were  
1734 measured as replicates and were made to fit a hyperbolic light-saturation curve (Larcher, 2003):

1735 
$$A_{20} = \left( \frac{Pm_{20} * PPFD}{\alpha_{PPFD} + PPFD} - R_{s20} \right) * B_{cap} \quad (B1)$$

1736 where subscript 20 denotes the variable value measured at 20 °C;  $R_s$  is the mass-based dark respiration rate

1737 ( $\mu\text{mol g}^{-1} \text{s}^{-1}$ );  $P_m$  is the mass-based rate of maximal gross photosynthesis ( $\mu\text{mol g}^{-1} \text{s}^{-1}$ ); and  $\alpha_{PPFD}$  is the  
 1738 half-saturation point ( $\mu\text{mol m}^{-2} \text{s}^{-1}$ ), i.e., PPFD level where half of  $P_m$  is reached. The measured  
 1739 morphological and photosynthetic traits are listed in Table 42.

1740

#### 1741 *Drying experiment*

1742 To link the water retention and photosynthesis of *Sphagnum* capitula, we performed a drying experiment  
 1743 using a GFS-3000 system to measure co-variations of capitulum water potential ( $h$ , cm water), water content  
 1744 ( $W_{cap}$ ,  $\text{g g}^{-1}$ ) and  $A$  ( $\mu\text{mol m}^{-2} \text{g}^{-1} \text{s}^{-1}$ ). For both species, four mesocosms were collected in August 2018 and  
 1745 transported to laboratory in UEF Joensuu, Finland. Capitula were harvested and wetted by water from the  
 1746 mesocosms. The capitula were then placed gently on a piece of tissue paper for 2 minutes and then placed  
 1747 into the same cuvette as used in the previous photosynthesis measurement. The cuvette was then placed  
 1748 into GFS and measured under constant conditions of  $PPFD$  ( $1500 \mu\text{mol m}^{-2} \text{s}^{-1}$ ), temperature ( $293.2\text{K}$ ),  
 1749 inflow air ( $700 \mu\text{mol s}^{-1}$ ),  $\text{CO}_2$  concentration ( $400 \text{ppm}$ ) and relative humidity ( $40\%$ ). Measurement was  
 1750 stopped when  $A$  dropped to less than  $10\%$  of its maximum. Each measurement lasted between  $120$  and  $180$   
 1751 minutes. Each sample was weighed before and after the gas-exchange measurement, then dried at  $40^\circ\text{C}$  for  
 1752  $48 \text{h}$  to determine the biomass of capitula ( $B_{cap}$ ).

1753 The GFS-3000 records the vapor pressure ( $e_a$ , kPa) and the evaporation rate ( $E$ ,  $\text{g s}^{-1}$ ) simultaneously with  
 1754  $A$  at [every second one hertz](#) (Heinz Walz GmbH, 2012). The changes in  $W_{cap}$  with time ( $t$ ) was calculated as  
 1755 following:

$$1756 \quad RWC(t) = (W_{pre} - B_c - \sum_{t=0}^t E(t)) / B_c \quad (\text{B2})$$

1757 We assumed that the vapor pressure at the surface of water-filled cells equaled the saturation vapor  
 1758 pressure ( $e_s$ ), and the vapor pressure in the headspace of cuvette equaled that in the outflow ( $e_a$ ). The vapor  
 1759 pressure in capitula pores ( $e_i$ ) thus can be calculated based on following gradient-transport function (Fig.  
 1760 B1A):

$$1761 \quad \lambda E(t) = \frac{\rho_a c_p (e_i(t) - e_a(t))}{\gamma r_a(t)} = \frac{\rho_a c_p (e_s - e_i(t))}{\gamma r_s(t)} \quad (\text{B3})$$

1762 where  $\lambda$  is the latent heat of vaporization;  $\gamma$  is the slope of the saturation vapor pressure - temperature  
 1763 relationship;  $r_a$  is the aerodynamic resistance ( $\text{m s}^{-1}$ ) for vapor transport from inter-leaf volume to  
 1764 headspace;  $r_s$  is the surface resistance of vapor transport from wet leaf surface to inter-leaf volume. The  
 1765 bulk resistance for evaporation ( $r_{bulk}$ ) was thus calculated as  $r_a + r_s$ .

1766 We assumed that the structures of tissues and pores did not change during the drying process and assumed  
 1767  $r_a$  to be constant during each measurement.  $A$  tended to increase with time  $t$  until it peaked ( $A_m$ ) and then  
 1768 decreased (Fig. 1B). The point  $A=A_m$  implied the water content where further evaporative loss would start  
 1769 to drain the cytoplasmic water, leading to the decrease in  $A$ . The response of  $A$  to  $W_{cap}$  was fitted as a  
 1770 second-order polynomial function (Robroek et al., 2009) using data from  $t_{Am}$  to  $t_n$ :

$$1771 \quad f_A(W_{cap}) = a_{w0} + a_{w1} * W_{cap} + a_{w2} * W_{cap}^2 \quad (\text{B4})$$

1772 where  $a_{w0}$ ,  $a_{w1}$  and  $a_{w2}$  are parameters; and  $f_A(W_{cap}) = A/A_m$ . For each replicate, the optimal water content



1773 for photosynthesis ( $W_{opt}$ ) was derived from the peak of fitted curve (Eq. 4). The capitulum water content at  
 1774 the compensation point  $W_{cmp}$ , where the rates of gross photosynthesis and respiration are equal, can be  
 1775 calculated from the point  $A=0$ .

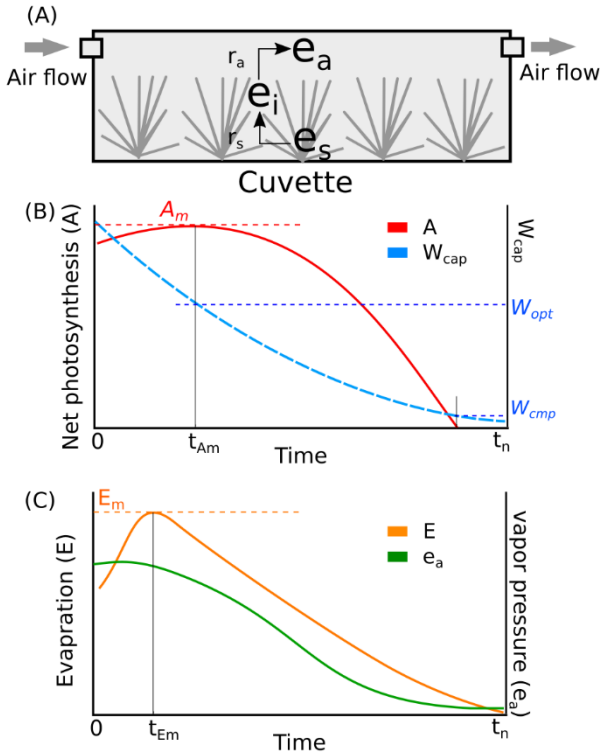


Figure B1. Conceptual schemes of (A) cuvette setting and resistances, (B) the co-variations of net photosynthesis and  $W_{cap}$ , and (C) the co-variations of evaporation and vapor pressure in headspace during a measurement. Meanings of symbols:  $e_a$ , vapor pressure in headspace of cuvette (kPa);  $e_i$ , vapor pressure in branch-leaf structure of capitula;  $e_s$ , vapor pressure at the surface of wet tissues;  $r_a$ , aerodynamic resistance of vapor diffusion from inner capitula to headspace;  $r_s$ , surface resistance of vapor diffusion from wet tissue surface to inner capitula space;  $A$ , net photosynthesis rate ( $\mu\text{mol m}^{-2} \text{s}^{-1}$ );  $A_m$ , maximal net photosynthesis rate ( $\mu\text{mol m}^{-2} \text{s}^{-1}$ );  $W_{cap}$ , water content of capitula ( $\text{g g}^{-1}$ );  $W_{opt}$ ,  $W_{cap}$  at  $A=A_m$ ;  $W_{cmp}$ ,  $W_{cap}$  at  $A=0$ ;  $E$ , evaporation rate ( $\text{mm s}^{-1}$ ).

1794

1795 Similarly, the evaporation rate ( $E$ ) increased from the start of measurement until maximum evaporation  
 1796  $E_m$ , and then decreased (Fig. B1C). The point  $E=E_m$  implied the time when the wet capitulum tissues were  
 1797 maximally exposed to the air flow. Therefore,  $r_a$  was estimated as the minimum of bulk resistance using  
 1798 Eq. (B5), by assuming  $e_i(t) \approx e_s$  when  $E(t) = E_m$ :

$$1799 \quad r_a = \frac{\rho_a c_p (e_s - e_a(t))}{\gamma \lambda E_m} \quad (\text{B5})$$

1800 Based on the calculated  $e_i(t)$ , we were able to derive the capitulum water potential ( $h$ ) following the  
 1801 equilibrium vapor-pressure method (e.g. Price et al, 2008; Goetz and Price, 2015):

$$1802 \quad h = \frac{RT}{Mg} \ln \left( \frac{e_i}{e_s} \right) + h_0 \quad (\text{B6})$$

1803 where  $R$  is the universal gas constant ( $8.314 \text{ J mol}^{-1} \text{ K}^{-1}$ );  $M$  the molar mass of water ( $0.018 \text{ kg mol}^{-1}$ );  $g$  is  
 1804 the gravitational acceleration ( $9.8 \text{ N kg}^{-1}$ );  $e_i/e_s$  is the relative humidity;  $h_0$  is the water potential due to the  
 1805 emptying of free-moving water before measurement (set to 10 kPa according to Hayward and Clymo,  
 1806 1982).

1807

1808 *Statistical analysis*

1809 The light response curve (Eq. B1) and the response function of  $A/A_m$  to  $W_{cap}$  changes (Eq. B4) were fitted  
1810 using nlme package in R **Studio** (version 3.1). The obtained values of shape parameters  $a_{w0}$ ,  $a_{w1}$  and  $a_{w2}$   
1811 (Eq. 4) were then used to calculate  $W_{opt}$  ( $W_{opt} = -0.5 a_{w1} / a_{w2}$ ) and  $W_{cmp}$  ( $W_{cmp} = 0.5 [-a_{w1} - (a_{w1}^2 - 4a_{w0} a_{w2})^{0.5}] / a_{w2}$ ). We then applied ANOVA to compare *S. magellanicum* against *S. fallax* for the traits obtained  
1812 from the field sampling (i.e. structural properties such as  $B_{cap}$ ,  $D_s$ ,  $H_{spc}$ ,  $W_{cf}$ ,  $W_{sf}$ ) and from the gas-exchange  
1813 measurements (i.e.  $Pm_{20}$ ,  $Rs_{20}$ ,  $W_{opt}$ ,  $W_{cmp}$  and  $r_{bulk}$ ), using R **Studio** (version 3.1).  
1814

1815 The measured values of capitulum water potential ( $h$ ) were  $\log_{10}$ -transformed and related to the variations  
1816 in  $W_{cap}$ ,  $B_{cap}$  and  $D_s$  with a linear model. Similarly, a linear model was established to quantify the response  
1817 of bulk resistance for evaporation ( $r_{bulk}$ ) ( $\log_{10}$ -transformed) to the variations in  $h$ ,  $B_{cap}$  and  $D_s$ . The linear  
1818 regressions were based on statsmodels (version 0.9.0) in Python (version 2.7), as supported by Numpy  
1819 (version 1.12.0) and Pandas (version 0.23.4) packages.

1820

## 1821 **Results of the empirical measurements**

1822 The two *Sphagnum* species differed in their structural properties (Table B1). Lawn species *S. fallax* had  
1823 looser structure than hummock species *S. magellanicum* as seen in lower capitulum density ( $D_s$ ) and  
1824 specific height ( $H_{spc}$ ) in *S. fallax* than in *S. magellanicum* ( $P < 0.05$ , Table. B1). Moreover, in conditions  
1825 prevailing in the study site *S. fallax* mosses were dryer than *S. magellanicum*; the field-water contents of *S.*  
1826 *fallax* capitulum ( $W_{cf}$ ) and stem ( $W_{sf}$ ) were 40% and 46% lower than *S. magellanicum* ( $P < 0.01$ , Table. B1),  
1827 respectively. The different density of capitulum of the two species differing in their capitulum size led to  
1828 similar capitulum biomass ( $B_{cap}$ ) ( $P = 0.682$ ) between *S. fallax* with small capitulum and *S. magellanicum*  
1829 with large capitulum. Unlike the structural properties, maximal  $CO_2$  exchange rates ( $Pm_{20}$  and  $Rs_{20}$ ) did not  
1830 differ between the two species (Table B1).

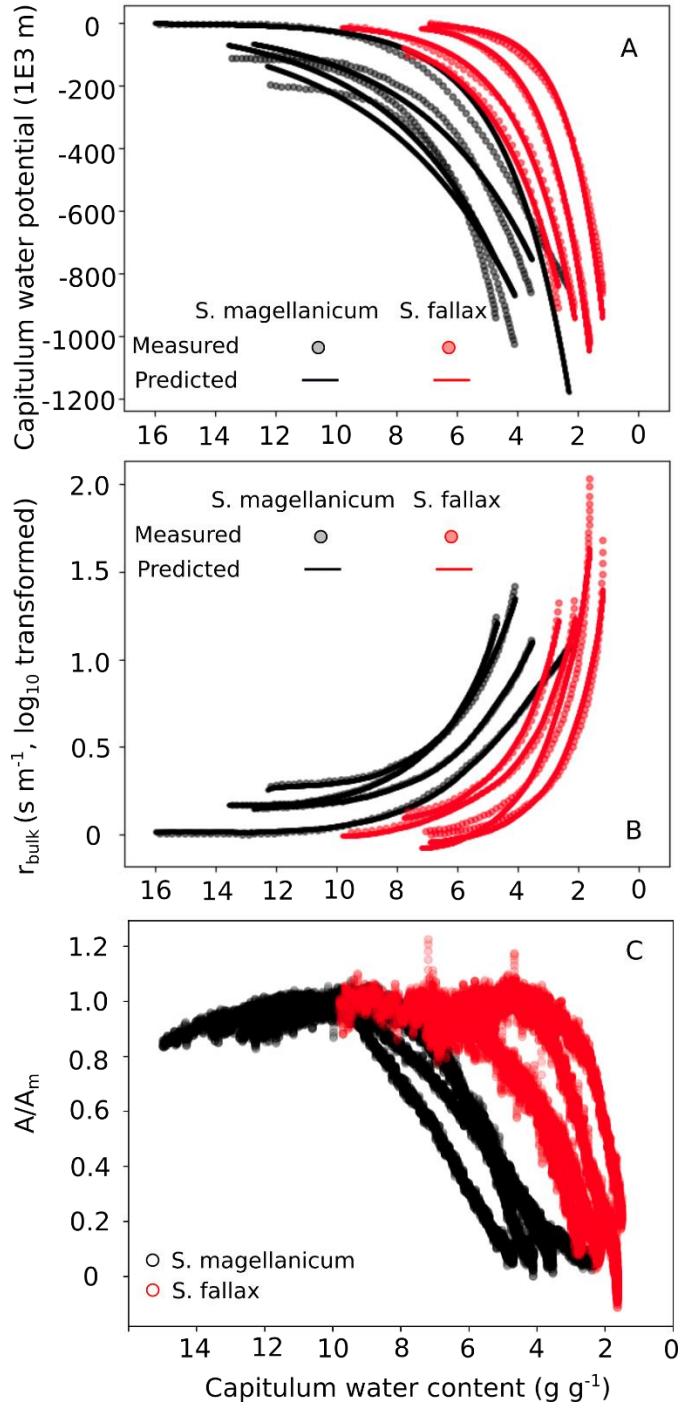
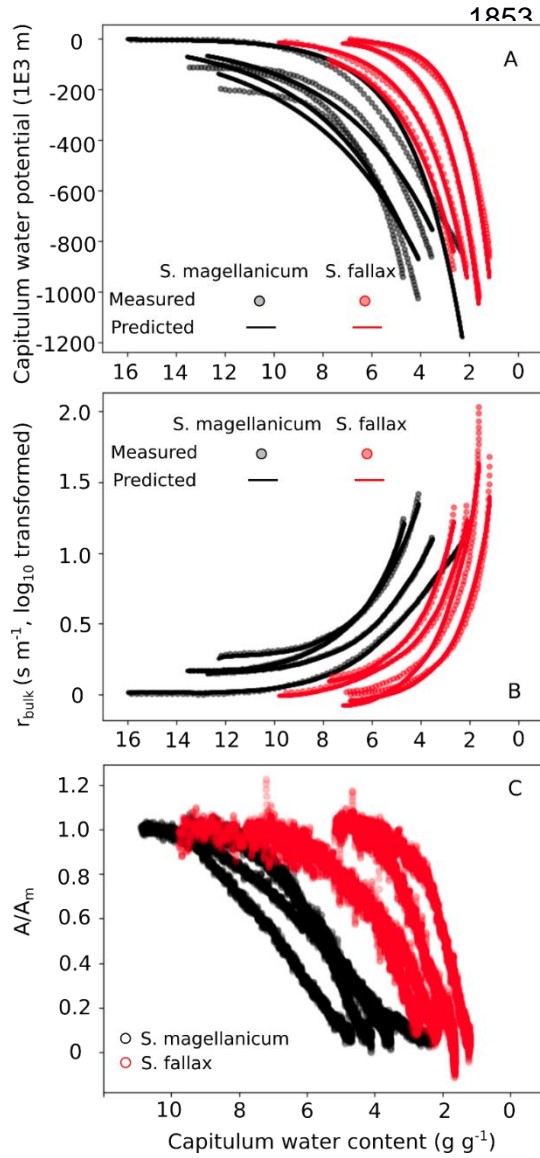
1831 The drying experiment demonstrated how capitulum water content regulated capitulum processes in both  
1832 studied *Sphagnum* species (Fig. B2). Decreasing capitulum water content ( $W_{cap}$ ) led to decrease in the water  
1833 potential ( $h$ ), the responses of  $h$  to  $W_{cap}$  varied among replicates (Fig. 2A). The values of  $W_{cap}$  for *S. fallax*  
1834 were generally lower than those for *S. magellanicum* under the same water potentials. The fitted linear  
1835 models explained over 95% of the variations in the measured  $h$  for both species (Table. B2), although fitted  
1836 responses of  $h$  to  $W_{cap}$  were slightly smoother than the measured ones, particularly for *S. magellanicum*  
1837 (Fig. B2A). The responses of  $h$  to  $W_{cap}$  was significantly affected by the capitulum density ( $D_s$ ), capitulum  
1838 biomass ( $B_{cap}$ ) and their interactions with  $W_{cap}$  (Table. B2).

1839 Decreasing capitulum water content ( $W_{cap}$ ), and water potential ( $h$ ), were associated with increasing bulk  
1840 resistance for evaporation ( $r_{bulk}$ , Fig. B2B), although the sensitivity of  $r_{bulk}$  to  $h$  changes varied by replicates.  
1841 The values of  $r_{bulk}$  from *S. fallax* were largely lower than those from *S. magellanicum* when the capitulum  
1842 water content of the two species were similar. The fitted linear models explained the observed variations in  
1843 the measured  $r_{bulk}$  well for both species (Fig. 2B and Table. B3). The variation in the response of  $r_{bulk}$  to  $h$   
1844 was significantly affected by capitulum density ( $D_s$ ), capitulum biomass ( $B_{cap}$ ) and their interactions with  
1845  $h$  (Table. B3).

1846 Decreasing capitulum water content ( $W_{cap}$ ) slowed down the net photosynthesis rate (Fig. B2C), as  
1847 represented by the decreasing ratio of  $A/A_m$ . *S. fallax* required lower capitulum water content ( $W_{cap}$ ) than

1848 *S. magellanicum* to reach photosynthetic maximum and photosynthetic compensation point. However, the  
 1849 ranges of capitulum water content from photosynthetic maximum ( $W_{opt}$ ) or field capacity ( $W_{fc}$ ) to that at  
 1850 compensation point ( $W_{cmp}$ ) were smaller for *S. fallax* than *S. magellanicum*. Hence, *S. fallax* had narrower  
 1851 transition zone for photosynthesis to respond to drying, compared to *S. magellanicum*.

1852



1854

1855  
1856  
1857  
1858  
1859  
1860  
1861  
1862  
1863  
1864  
1865  
1866  
1867  
1868  
1869  
1870  
1871  
1872  
1873

Figure B2. Responses of (A) capitulum water potential, (B) bulk resistance of evaporation, and (C) net photosynthesis to changes in capitulum water content ( $W_{cap}$ ) of two *Sphagnum* species typical to hummocks (*S. magellanicum*, black) and lawns (*S. fallax*, red). As the measured results are based on the drying experiment starting with fully wetted capitula characteristic for both species, the X-axis is shown from high to low  $W_{cap}$ . The values predicted in (B) and (C) are based on linear models with parameter values listed in Tables B2 and B3 and predictor values from the drying experiment.

1874 Table. B1 Species-specific traits of morphological, photosynthetic and water-retention from *S. magellanicum* and *S.*  
1875 *fallax*. Trait values (mean  $\pm$  standard deviation) and ANOVA statistics F- and p-values are given for comparing the  
1876 means of traits of the two species.

Trait	<i>S. magellanicum</i>	<i>S. fallax</i>	F	P (>F)
Capitulum density, $D_S$ (capitula cm <sup>-2</sup> )	0.922 $\pm$ 0.289	1.46 $\pm$ 0.323	6.224 <sup>a</sup>	0.037 *
Capitulum biomass, $B_{cap}$ (g m <sup>-2</sup> )	75.4 $\pm$ 21.5	69.2 $\pm$ 19.6	0.181 <sup>a</sup>	0.682
Specific height, $H_{spc}$ (cm g <sup>-1</sup> m <sup>-2</sup> )	45.4 $\pm$ 7.64	32.6 $\pm$ 6.97	6.126 <sup>a</sup>	0.038*
Field water content of capitula, $W_{cf}$ (g g <sup>-1</sup> )	14.7 $\pm$ 3.54	8.09 $\pm$ 1.48	11.75 <sup>a</sup>	0.009**
Field water content of stems, $W_{sf}$ (g g <sup>-1</sup> )	18.4 $\pm$ 1.92	10.2 $\pm$ 1.50	45.81 <sup>a</sup>	0.0001**
Maximal gross photosynthesis rate at 20 °C, $Pm_{20}$ ( $\mu$ mol g <sup>-1</sup> s <sup>-1</sup> )	0.019 $\pm$ 0.004	0.014 $\pm$ 0.002	3.737 <sup>b</sup>	0.101
Respiration rate at 20 °C, $Rs_{20}$ ( $\mu$ mol g <sup>-1</sup> s <sup>-1</sup> )	0.007 $\pm$ 0.004	0.007 $\pm$ 0.002	0.012 <sup>b</sup>	0.92
half-saturation point of photosynthesis, $\alpha_{PPFD}$ ( $\mu$ mol g <sup>-1</sup> s <sup>-1</sup> )	101.4 $\pm$ 14.1	143 $\pm$ 51.2	2.856 <sup>b</sup>	0.142

Optimal capitulum water content for photosynthesis, $W_{opt}$ (g g <sup>-1</sup> )	9.41±0.73	5.81±1.68	11.57 <sup>b</sup>	0.0145*
Capitulum water content at photosynthetic compensation point, $W_{cmp}$ (g g <sup>-1</sup> )	3.67±0.83	1.78±0.43	12.35 <sup>b</sup>	0.0126*
Minimal bulk resistance of evaporation, $r_a$ (m s <sup>-1</sup> )	33.5±7.30	40.7±4.99	1.976 <sup>b</sup>	0.2165

1877 <sup>a</sup> soil-core measurement, sample  $n=5$ ; <sup>b</sup> cuvette gas-exchange measurement, sample  $n=4$ ; \* the difference of means is  
1878 significant ( $P<0.05$ ); \*\* the difference of means is very significant ( $P<0.01$ ).  
1879

1880 Table B2. Parameter estimates of the linear model for the log<sub>10</sub>-transformed capitulum water potential ( $h$ ) for *S. fallax*  
1881 and *S. magellanicum*. Estimate value, standard error (SE), and test statistics p-values are given to the predictors of the  
1882 models. Predictors are: capitulum biomass ( $B_{cap}$ ), capitulum density ( $D_S$ ), capitulum water content ( $W_{cap}$ ), the  
1883 interaction of capitulum biomass and water potential ( $B_{cap} \times W_{cap}$ ), the interactions of capitulum biomass and capitulum  
1884 density ( $D_S \times W_{cap}$ ), the interactions of capitulum density and water potential ( $D_S \times W_{cap}$ ), and the interaction of  
1885 capitulum biomass, capitulum density and water potential ( $B_{cap} \times D_S \times W_{cap}$ ). All coefficient values are significantly  
1886 different from 0 ( $p<0.001$ ).

Parameter	<i>S. magellanicum</i> (R <sup>2</sup> =0.972)		<i>S. fallax</i> (R <sup>2</sup> =0.984)	
	Value	SE	Value	SE
(Intercept)	25.30	0.253	-90.99	2.158
$B_{cap}$	-272.10	3.133	2294.67	52.342
$W_{cap}$	-9.50	0.031	-62.12	0.600
$B_{cap} \times W_{cap}$	114.61	0.387	1500.26	14.549
$D_S$	-21.76	0.253	104.11	2.376
$B_{cap} \times D_S$	268.95	3.112	-2422.79	55.251
$D_S \times W_{cap}$	9.33	0.031	68.35	0.661
$B_{cap} \times D_S \times W_{cap}$	-113.33	0.386	-1588.06	15.360

1887

1888 Table B3. Parameter estimates of the linear model for the log<sub>10</sub>-transformed capitulum evaporative resistance ( $r_{bulk}$ )  
 1889 for *S. fallax* and *S. magellanicum*. Estimate value, standard error (SE), and test statistics p-values are given to the  
 1890 predictors of the models. Predictors are: capitulum biomass ( $B_{cap}$ ), capitulum density ( $D_S$ ), water potential ( $h$ ), the  
 1891 interaction of capitulum biomass and water potential ( $B_{cap} \times h$ ), the interactions of capitulum biomass and capitulum  
 1892 density ( $D_S \times h$ ), the interactions of capitulum density and water potential ( $D_S \times h$ ), and the interaction of capitulum  
 1893 biomass, capitulum density and water potential ( $B_{cap} \times D_S \times h$ ). All coefficient values are significantly different from 0  
 1894 ( $p < 0.001$ ).

Parameter	<i>S. magellanicum</i> (R <sup>2</sup> =0.998)		<i>S. fallax</i> (R <sup>2</sup> =0.966)	
	Value	SE	Value	SE
(Intercept)	-1.13	0.027	55.07	2.225
$B_{cap}$	14.45	0.334	1334.55	53.968
$h$	0.0012	5.92e-05	-0.028	0.004
$B_{cap} \times h$	-0.0007	0.001	0.707	0.101
$D_S$	1.08	0.027	-60.53	2.450
$B_{cap} \times D_S$	-13.39	0.333	1406.36	56.968
$D_S \times h$	0.0002	5.89e-05	0.0317	0.005
$B_{cap} \times D_S \times h$	-0.0017	0.001	-0.733	0.106

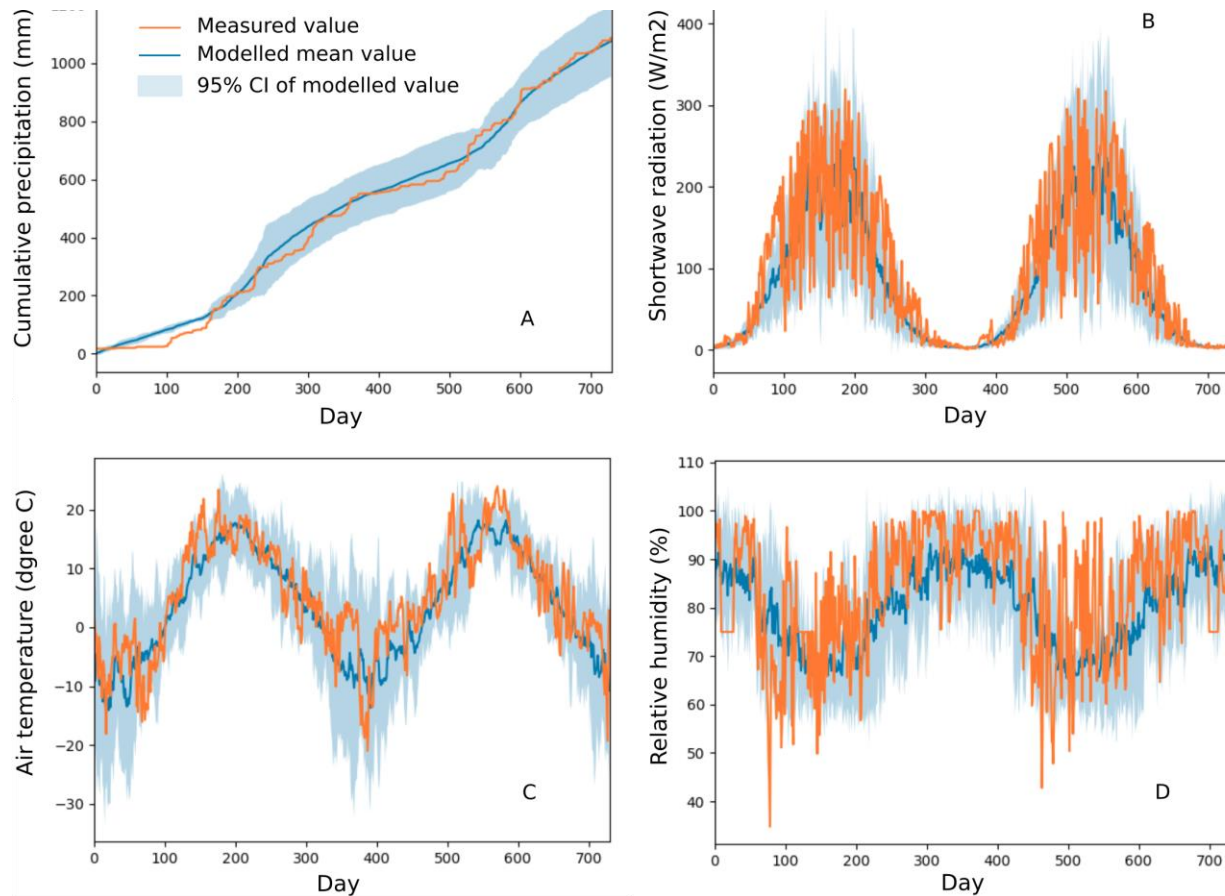
1895  
 1896  
 1897 References  
 1898 Goetz, J. D. and Price, J. S.: Role of morphological structure and layering of *Sphagnum* and *Tomenthypnum*  
 1899 mosses on moss productivity and evaporation rates, Canadian Journal of Soil Science, 95, 109-124, 2015.  
 1900 Hayward P. M. and Clymo R. S.: Profiles of water content and pore size in *Sphagnum* and peat, and their  
 1901 relation to peat bog ecology. Proceedings of the Royal Society of London, Series B, Biological Sciences,  
 1902 215, 299-325, 1982.  
 1903 Korrensalo, A., Alekseychik, P., Hájek, T., Rinne, J., Vesala, T., Mehtätalo, L., Mammarella, I. and Tuittila,  
 1904 E.-S.: Species-specific temporal variation in photosynthesis as a moderator of peatland carbon  
 1905 sequestration, Biogeosciences, 14, 257-269, 2017.  
 1906 [Laine, A. M., Juurola, E., Hájek, T., & Tuittila, E. S.: \*Sphagnum\* growth and ecophysiology during mire](#)  
 1907 [succession. \*Oecologia\*, 167\(4\), 1115-1125, 2011.](#)  
 1908 [Laine, A. M., Ehonen, S., Juurola, E., Mehtätalo, L., & Tuittila, E. S.: Performance of late succession](#)  
 1909 [species along a chronosequence: Environment does not exclude \*Sphagnum fuscum\* from the early stages of](#)  
 1910 [mire development. \*Journal of vegetation science\*, 26\(2\), 291-301, 2015.](#)  
 1911 Larcher, W.: Physiological Plant Ecology: Ecophysiology and Stress Physiology of Functional Groups,  
 1912 Springer, 2003.  
 1913 Price, J. S., Whittington, P. N., Elrick, D. E., Strack, M., Brunet, N. and Faux, E.: A method to determine  
 1914 unsaturated hydraulic conductivity in living and undecomposed moss, Soil Sci. Soc. Am. J., 72, 487 – 491,  
 1915 2008.  
 1916 Robroek, B. J.M., Schouten, M. G.C., Limpens, J., Berendse, F. and Poorter, H.: Interactive effects of water

1917 table and precipitation on net CO<sub>2</sub> assimilation of three co-occurring Sphagnum mosses differing in  
1918 distribution above the water table, *Global Change Biology* 15, 680 – 691, 2009.



1919 **Appendix C. Comparisons of meteorological variables simulated by Weather Generator and those**  
 1920 **measured from Siikaneva peatland site (ICOS site located in 10 km distance from the study site**  
 1921 **Lakkasuo)**

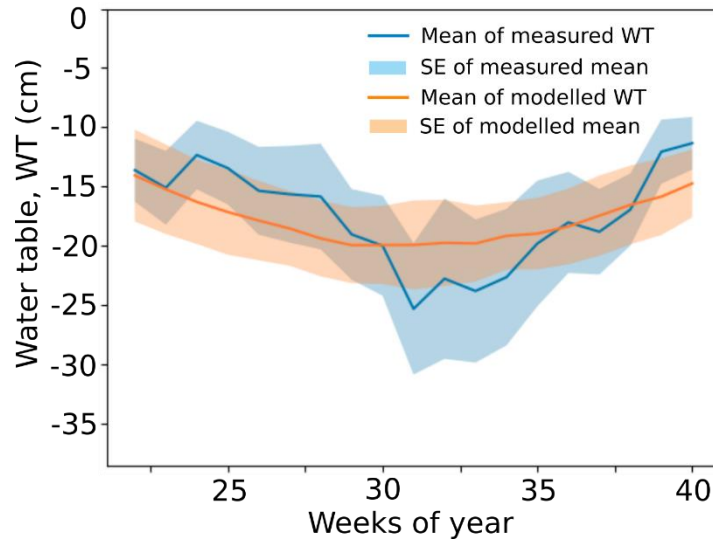
1922



1923 Fig. C1 Comparisons of meteorological variables simulated by Weather Generator and those measured  
 1924 from Siikaneva peatland site. The variables include (A) cumulative precipitation (mm), (B) incoming  
 1925 shortwave radiation ( $W m^{-2}$ ), (C) air temperature ( $^{\circ}C$ ), and (D) relative humidity (%). These variables were  
 1926 measured and simulated at half-hourly timescale. The measurements were carried out during 2012-2013.  
 1927 Details about the site and measurements have been described by Alekseychik et al. (2018). The measured  
 1928 seasonal dynamics of the meteorological variables were generally in line with the 95% confidence intervals  
 1929 (CI) of the simulated values, which were calculated based on Monte-Carlo simulations ( $n=5$ ).

1930

1931 **Appendix D. Comparisons of seasonal water table measured from the study site and the values**  
1932 **simulated based on calibrated net inflow**



1933

1934 Fig. D1 Comparison of seasonal water table (WT) measured at the Lakkasuo study site and the values  
1935 simulated by the calibrated PCS. WT values were sampled weekly from the lawn habitats both in field and  
1936 in model output. The weekly mean WT was measured during 2001, 2002, 2004 and 2016. The modelled  
1937 means and standard deviations (SD) of WT were based on 20 Monte-Carlo simulations. The simulated  
1938 seasonality of mean WT generally followed the measured trends. The calibration reduced the sum of  
1939 squared error (*SE*, Eq. 12) from 199.5 ( $a_N=b_N=0$ ) to 117.3. The calibrated values for  $a_N$  and  $b_N$  were -  
1940  $5.3575 \cdot 10^{-4}$  and  $4.7599 \cdot 10^{-5}$ , respectively (Eq. A18).